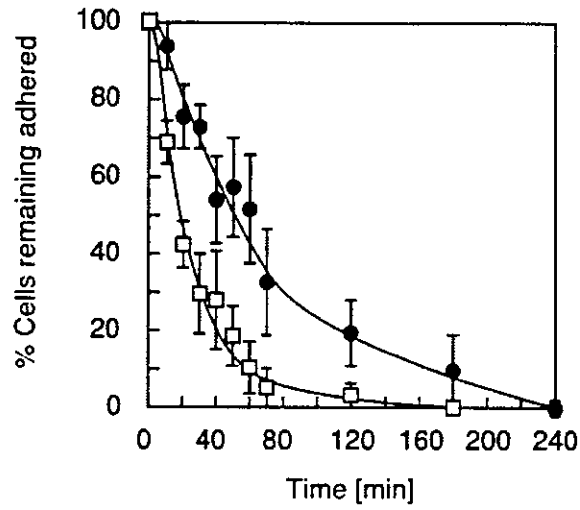

Figure 4. Time-dependent cell detachment from PIPAAm- and IB5-grafted surfaces by low temperature treatment at 20°C after 48-h culture at 37°C. Data are expressed as the mean with standard error of mean (n = 3). Initial seeded cell density: 1 × 10^4 cells/cm^2. Open square, PIPAAm; filled circle, IB5.

surfaces [Fig.3(b)]. Hydrophobic BMA components suppressed PIPAAm hydration at this temperature, promoting cell adhesion on IB5-grafted surfaces. This indicated that culture temperatures promoting cell adhesion could be reduced and regulated by copolymerizing with the hydrophobic monomer, BMA.

Single-cell detachment by low temperature treatments

After 48-h culture at 37°C, seeded BAECs adhered well and showed spread morphologies on both PIPAAm- and IB5-grafted surfaces. Cell adhesion on those dishes was nearly identical with that on TCPS dishes (data not shown). Culture temperature was then reduced to 20°C and cell detachment from the PIPAAm- and IB5-grafted dishes were observed. No cell detachment was observed from TCPS surfaces within the examined time ranges up to 24 h. Figure 4 shows time dependence for cells remaining adherent on surfaces. In detachment, individual cells spontaneously changed their shape from a spread to a round form without any enzymatic treatment, and finally cultured cells detached completely from both PIPAAm- and IB5-grafted surfaces. A majority of cells (ca. 90%) detached within 1 h, then, 3 h after incubation at 20°C, all cells were detached from PIPAAm-grafted dishes. However, another 1-h incubation was required for complete cell detachment from IB5-grafted dishes because hydrophobic BMA molecules in the copolymer reduce the copolymer hydrophilicity to reduce surface hydration and resulting cell lifting. These results clearly demonstrate that the grafted polymer hydration significantly influences cell–materials interaction, namely, more hydrophobic surfaces decelerate cell lifting. A discrepancy between surface wettability and cell detachment from IB5-grafted surfaces can be seen by comparing data in Figures 2 and 4. Namely, cells detached even though IB-5 surfaces remain hydrophobic state at 20°C from the data in Figure 2. In cell detachment experiments, polymer-grafted surfaces were always exposed to aqueous medium at 37°C during cell adhesion. By contrast, contact angles were measured on dry polymer-grafted surface samples. Such differences may influence the observed discrepancy. By lowering temperature, IPAAm sequences in surface grafted IB5 chains become hydration, although the degree is small as hydrophobic BMA units suppress complete hydration as was seen for PIPAAm-grafted surfaces. Such a hydration on IPAAm sequences may effect to cell detachment process from IB5-grafted surfaces upon reducing temperature to 20°C.[33] Cell attachment and detachment are thus controllable by regulating BMA content in the grafted copolymers.

Cell sheet detachment from grafted surfaces

In our previous reports,[17,19] enzyme-free harvest of confluently cultured cell monolayers was achieved in tissue-like cell sheets by only lowering culture temperatures to 20°C, altering surface properties to hydrophilic. Here, temperature-dependent spontaneous cell sheet detachment was investigated on copolymer grafted surfaces to examine influences of copolymer composition. Seeded BAECs on PIPAAm, IBX-grafted, and control TCPS surfaces readily adhered and proliferated in serum media, reaching confluence with cell–cell junction formation at 37°C without precoating of adhesive ECM proteins. Cell adhesion and spreading on these surfaces 4 days after seeding were identical in both morphologies and cell densities. These dishes were then transferred into CO_2 incubators adjusted either to 28, 25, or 20°C. Cell monolayer sheet detachment processes from both PIPAAm- and IB5-grafted surfaces were photographed over time and shown in Figure 5. Detachment was basically similar for all grafted surfaces as indicated in Figure 5 and reported previously.[17-21] First, cultured cell monolayers start detaching spontaneously from the edges of (co)polymer-grafted surfaces [Fig. 5(b) and (e)] accompanying the surface property alteration. Then cell sheets gradually lift off with accompanying sheet shrinkage and agglomeration. They finally completely detach as a single piece from the modified surfaces and float in the medium [Fig. 5(c) and (f)].

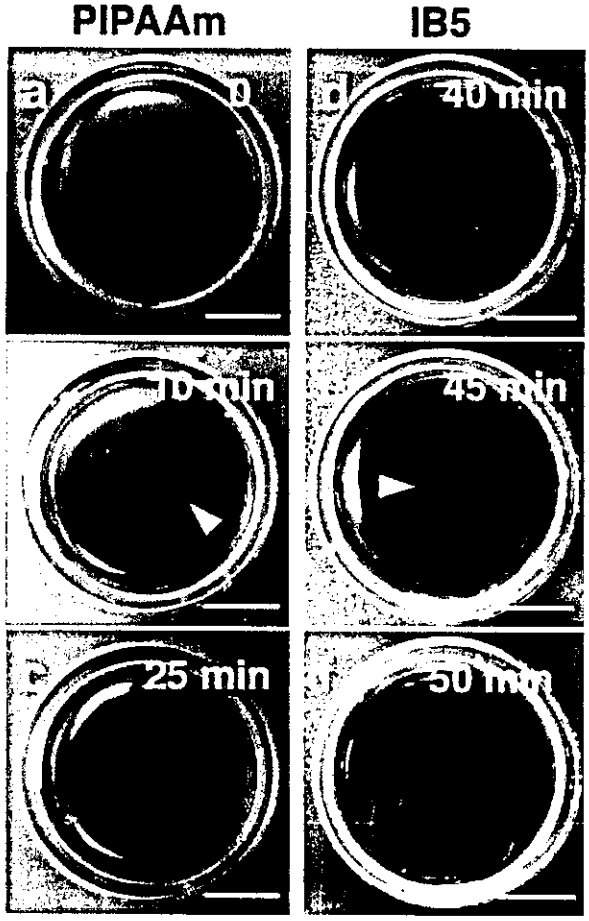

Figure 5. Macroscopic view of time-dependent detachment of confluent cultures of endothelial cells from PIPAAm-grafted (a–c) and IB5-grafted (d–f) surfaces at 20°C, showing both detached and adherent portions of BAEC monolayers. PIPAAm-grafted surface: (a) 0; (b) 10; and (c) 25 min, IB5-grafted surface: (d) 40; and (e) 45; and (f) 50 min after incubation at 20°C. Scale bar = 1 cm.

Contraction of recovered cell sheets is probably due to the disappearance of anchorage-dependence caused by surface hydration, and to the strong cell–cell interactions within the sheet. From the photographs acquired during detachment processes at different temperatures, areal changes in cells remaining adherent on these thermoresponsive surfaces were digitized on NIH Image software over time.

Figure 6 shows time-dependent areal changes of cell monolayers for thermoresponsive surfaces at three low-temperature conditions. Cells on control TCPS surfaces remain adherent regardless of temperature and time (data not shown). It is clear that recovery of cell sheets and time required for complete sheet detachment are closely related to the composition of surface-grafted polymers and treatment temperatures. At any treatment temperature, longer incubation times were required to complete cell detachment with increasing BMA content in the copolymers. Cell sheet detachment was accelerated by reducing temperature from 28 to 20°C. At 28°C, detachment of cell monolayers was observed from only PIPAAm- and IB1-grafted surfaces, while no cell monolayers detached from either IB3- and IB5-grafted surfaces within the examined time ranges to 24 h. IB3- and IB5-grafted surfaces remained hydrophobic at this temperature, allowing cells to remain adhered on the modified surfaces. In sharp contrast, PIPAAm- and IB1-grafted surfaces became hydrophilic through hydration of grafted polymer molecules, promoting cell detachment from the hydrated surfaces at 28°C. Further low-temperature treatment at 25 and 20°C allows accelerated cell sheet detachment from all surface types. Complete cell sheet detachment occurred from IB1-grafted surfaces after 60-min incubation at 28°C, while only 30-min incubation is necessary at 20°C. Similarly, while cell sheets remained adherent on IB5-grafted surfaces at 28°C, they were completely recovered in 150 min at 25°C and in 50 min at 20°C, respectively.

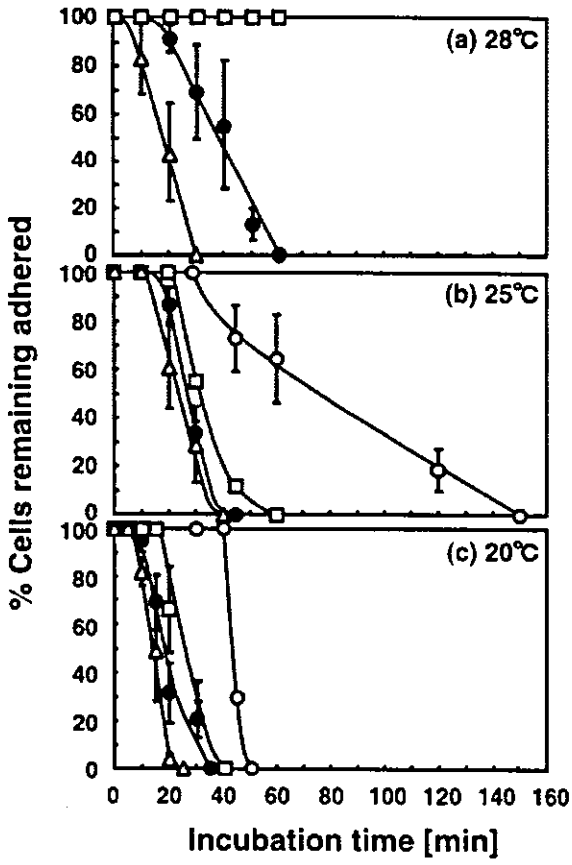

Figure 6. Time-dependent cell sheet area remaining adherent on PIPAAm-, and IBX-grafted surfaces: Open triangle, PIPAAm; filled circle, IB1; open square, IB3; open circle, IB5 at various temperature: (a) 28°C; (b) 25°C; (c) 20°C. Data are expressed as the mean with standard error of mean (n = 3–5).

Cell sheet detachment process and required times for complete cell sheet detachment are dependent on modifier characteristics as well as temperature treated. Detachment rate was almost identical for all samples once cell detachment initiated from the periphery of cell monolayer at either 20 or 25°C except for IB5 at 25°C, although starting time for cell sheet detachment retarded with increasing BMA content in the copolymer. Hydration of surface grafted polymers may play crucial role at the beginning of cell sheet detachment, the more hydrophilic polymers were grafted on the surfaces, the faster initial cell detachment at the periphery was observed. Once cell sheet periphery detached, cell-to-cell interactions and contraction facilitate whole cell-sheet detachment. Therefore, almost identical detachment rate was observed regardless of polymer types.

With increasing BMA content in the copolymers, time required for cell sheet detachment was extended. Low-temperature treatment for longer time periods would deteriorate cellular metabolic functions. Kwon et al.[34] grafted PIPAAm onto porous membranes and succeeded in accelerating cultured cell monolayer detachment with low-temperature treatment by allowing rapid PIPAAm hydration through increased thermal and water transport. Higher cell-sheet detachment rates are therefore expected by grafting IBX onto porous membranes[34] and/or cografting with poly(ethylene glycol),[35] known also to promote rapid hydration and more dynamic polymer molecular motion. Furthermore, cell monolayers can be recovered without cell sheet aggolemeration and permitting transfer to other surfaces with hydrophilic poly(vinylidene difluoride) (PVDF) support membranes as reported in elsewhere.[19,20,36]

The present research reveals that cell detachment temperature can be modulated below 32°C by introducing BMA as the hydrophobic component to PIPAAm. Through a patterned grafting technique,[22,23] spatial cell arrangements with two cell types and thermal recovery can now be performed using spatial patterns grafting different thermoresponsive polymers. Such a strategy can be applied to construct more complicated tissues through cell sheet engineering technologies. Pattern coculture of two cell types on such patterned surfaces with different thermal responses will be presented in forthcoming separate technical reports.

CONCLUSIONS

A hydrophobic monomer, BMA, was incorporated into PIPAAm and grafted onto TCPS dishes by electron beam irradiation. Changes in BMA content in the copolymers resulted in regulation of both surface wettability transition temperatures and the magnitude of wettability changes. These surface property alterations with BMA play important roles in cell adhesion/detachment control at various temperatures. The present surface modification technique should prove useful for recovery of two-dimensional cocultured cell sheets with surfaces pattern-grafted with PIPAAm and copolymers for tissue engineering applications, as well as basic research in cell–cell communication and coculture *in vitro*.

The authors are grateful to Professor David W. Grainger, Colorado State University, for his valuable comments and discussions throughout the research.

References

1. Heskins M, Guillent JE, James E. Solution properties of poly(*N*-isopropylacrylamide). J Macromol Sci Chem 1968;A2:1441–1445.
2. Bae YH, Okano T, Kim SW. Temperature dependence of swelling of crosslinked poly(*N,N'*-alkyl substituted acrylamides) in water. J Polym Sci Polym Phys 1990;28:923–936.
3. Bae YH, Okano T, Kim SW. "On–off" thermocontrol of solute transport I. Temperature dependence of swelling on *N*-isopropylacrylamide networks modified with hydrophilic components in water. Pharmaceut Res 1991;8:531–537.
4. Bae YH, Okano T, Kim SW. "On–off" thermocontrol of solute transport II. Solute release from thermosensitive hydrogels. Pharmaceut Res 1991;8:624–628.
5. Kanazawa H, Yamamoto K, Matsushima Y, Takai N, Kikuchi A, Sakurai Y, Okano T. Temperature-responsive chromatography using poly(*N*-isopropylacrylamide)-modified silica. Anal Chem 1996;68:100–105.
6. Kanazawa H, Kashiwase Y, Yamamoto K, Matsushima Y, Kikuchi A, Sakurai Y, Okano T. Temperature-responsive liquid chromatography. 2. Effects of hydrophobic groups in *N*-isopropylacrylamide copolymer-modified silica. Anal Chem 1997;69:823–830.
7. Kikuchi A, Okano T. Intelligent thermoresponsive polymeric stationary phase for aqueous chromatography of biological compounds. Prog Polym Sci 2002;27:1165–1193.
8. Malmstadt N, Yager P, Hoffman AS, Stayton PS. A smart microfluidic affinity chromatography matrix composed of poly(*N*-isopropylacrylamide)-coated beads. Anal Chem 2003;75:2943–2949.
9. Stayton PS, Shimoboji T, Long C, Chilkoti A, Chen G, Harris JM, Hoffman AS. Control of protein-ligand recognition using a stimuli-responsive polymer. Nature 1995;378:472–474.
10. Matsukata M, Aoki T, Sanui K, Ogata N, Kikuchi A, Sakurai Y, Okano T. Effect of molecular architecture of poly(*N*-isopropylacrylamide)-trypsin conjugates on their solution and enzymatic properties. Bioconjugate Chem 1996;7:96–101.
11. Ding Z, Long CJ, Hayashi Y, Bulmus EV, Hoffman AS, Stayton PS. Temperature control of biotin binding and release with a streptavidin-poly(*N*-isopropylacrylamide) site-specific conjugate. Bioconjugate Chem 1999;10:395–400.
12. Hoffman AS, Stayton PS, Bulmus V, Chen G, Chen J, Cheung C, Chilkoti A, Ding Z, Dong L, Fong R, Lackey CA, Long CJ, Press OW, Shimoboji T, Shoemaker S, Yang HJ, Monji N, Nowinski RC, Cole CA, Priest JH, Harris JM, Nakamae K, Nishino T, Miyata T. Really smart bioconjugates of smart poly-

mers and receptor proteins. J Biomed Mater Res 2000;52:577–586.
13. Yamada N, Okano T, Sakai H, Karikusa F, Sawasaki Y, Sakurai Y. Thermo-responsive polymer surfaces; Control of attachment and detachment of cultured cells. Makromol Chem Rapid Commun 1990;11:571–576.
14. Okano T, Yamada N, Sakai H, Sakurai Y. A novel recovery system for cultured cells using plasma-treated polystyrene dishes grafted with poly(*N*-isopropylacrylamide). J Biomed Mater Res 1993;27:1243–1251.
15. Okano T, Yamada N, Okuhara M, Sakai H, Sakurai Y. Mechanisim of cell detachment from temperature-modulated, hydrophilic-hydrophobic polymer surfaces. Biomaterials 1995;16:297–303.
16. Sakai H, Doi Y, Okano T, Yamada N, Sakurai Y. Thermo-responsive polymer surfaces for cell culture: Analysis of the surfaces and control of the cell attachment/detachment. In Ogata N, SW Kim, Feijen J, Okano T, editors. Advanced biomaterials in biomedical engineering and drug delivery systems. Tokyo: Springer-Verlag; 1996. p 229–230.
17. Kushida A, Yamato M, Konno C, Kikuchi A, Sakurai Y, Okano T. Decrease in culture temperature releases monolayer endothelial cell sheets together with deposited fibronectin matrix from temperature-responsive culture surfaces. J Biomed Mater Res 1999;45:355–362.
18. Kikuchi A, Okuhara M, Karikusa F, Sakurai Y, Okano T. Two-dimensional manipulation of confluently cultured vascular endothelial cells using temperature-responsive poly(*N*-isopropylacrylamide)-grafted surfaces. J Biomater Sci Polym Ed 1998;9: 1331–1348.
19. Hirose M, Kwon OH, Yamato M, Kikuchi A, Okano T. Creation of designed shape cell sheets that are noninvasively harvested and moved onto another surface. Biomacromolecules 2000;1: 377–381.
20. Harimoto M, Yamato M, Hirose M, Takahashi C, Isoi Y, Kikuchi A, Okano T. Novel approach for achieving double-layered cell sheets co-culture: Overlayering endothelial cell sheets onto monolayer hepatocytes utilizing temperature-responsive culture dishes. J Biomed Mater Res 2002;62:464–470.
21. Shimizu T, Yamato M, Isoi Y, Akutsu T, Setomaru T, Abe K, Kikuchi A, Umezu M, Okano T. Fabrication of pulsatile cardiac tissue grafts using a novel 3-dimensional cell sheet manipulation technique and temperature-responsive cell culture surfaces. Circ Res 2002;90:e40–e48.
22. Yamato M, Kwon OH, Hirose M, Kikuchi A, Okano T. Novel patterned cell coculture utilizing thermally responsive grafted polymer surfaces. J Biomed Mater Res 2001;55:137–140.
23. Yamato M, Konno C, Utsumi M, Kikuchi A, Okano T. Thermally responsive polymer-grafted surfaces facilitate patterned cell seeding and co-culture. Biomaterials 2002;23:561–567.
24. Takei YG, Aoki T, Sanui K, Ogata N, Okano T, Sakurai Y. Temperature-responsive bioconjugates. 2. Molecular design for temperature-modulated bioseparations. Bioconjugate Chem 1993;4:341–346.
25. Iwata H, Oodate M, Uyama Y, Amemiya H, Ikada Y. Preparation of temperature-sensitive membranes by graft polymerization onto a porous membrane. J Membr Sci 1991;55:119–130.
26. Feil H, Bae YH, Feijen J, Kim SW. Effect of comonomer hydrophilicity and ionization on the lower critical solution temperature of *N*-isopropylacrylamide copolymers. Macromolecules 1993;26:2496–2500.
27. van Wachem PB, Beugeling T, Feijen J, Bantjes A, Detmers JP, van Aken WG. Interaction of cultured human endothelial cells with polymeric surfaces with different wettabilities. Biomaterials 1985;6:403–408.
28. van Wachem PB, Hogt AH, Beugeling T, Feijen J, Bantijes A, Detmers JP, van Aken WG. Adhesion of cultured human endothelial cells onto methacrylate polymers with varying surface wettability and charge. Biomaterials 1987;8:323–328.
29. Lee JH, Park JW, Lee HB. Cell adhesion and growth on polymer surfaces with hydroxyl groups prepared by water vapour plasma treatment. Biomaterials 1991;12:443–448.
30. Tamada Y, Ikada Y. Fibroblast growth on polymer surfaces and biosynthesis of collagen. J Biomed Mater Res 1994;28:783–789.
31. Takei YG, Aoki T, Sanui K, Ogata N, Sakurai Y, Okano T. Dynamic contact angle measurement of temperature-responsive surface properties for poly(*N*-isopropylacrylamide) grafted surfaces. Macromolecules 1994;27:6163–6166.
32. Yakushiji T, Sakai K, Kikuchi A, Aoyagi T, Sakurai Y, Okano T. Graft architectural effects on thermoresponsive wettability changes of poly(*N*-isopropylacrylamide)-modified surfaces. Langmuir 1998;14:4657–4662.
33. Dong L, Hoffman AS. A novel approach for preparation of pH-sensitive hydrogels for enteric drug delivery. J Controlled Release 1991;15:141–152.
34. Kwon OH, Kikuchi A, Yamato M, Sakurai Y, Okano T. Rapid cell sheet detachment from poly(*N*-isopropylacrylamide)-grafted porous cell culture membranes. J Biomed Mater Res 2000;50:82–89.
35. Kwon OH, Kikuchi A, Yamato M, Okano T. Accelerated cell sheet recovery by co-grafting of PEG with PIPAAm onto porous cell culture membranes. Biomaterials 2003;24:1223–1232.
36. Kushida A, Yamato M, Kikuchi A, Okano T. Two-dimensional manipulation of differentiated Madin-Darby canine kidney (MDCK) cell sheets: The noninvasive harvest from temperature-responsive culture dishes and transfer to other surfaces. J Biomed Mater Res 2001;54:37–46.

Temperature-Responsive Cell Culture Surfaces Enable "On−Off" Affinity Control between Cell Integrins and RGDS Ligands

Mitsuhiro Ebara,† Masayuki Yamato,‡ Takao Aoyagi,‡ Akihiko Kikuchi,‡ Kiyotaka Sakai,† and Teruo Okano*,‡

Department of Applied Chemistry, Waseda University, 3-4-1 Ohkubo, Shinjuku-ku, Tokyo 169-8555, Japan, and Institute of Advanced Biomedical Engineering and Science, Tokyo Women's Medical University, 8-1 Kawada-cho, Shinjuku-ku, Tokyo 162-8666, Japan

Received September 16, 2003; Revised Manuscript Received December 9, 2003

In this study, specific interactions between immobilized RGDS (Arg-Gly-Asp-Ser) cell adhesion peptides and cell integrin receptors located on cell membranes are controlled in vitro using stimuli-responsive polymer surface chemistry. Temperature-responsive poly(*N*-isopropylacrylamide-*co*-2-carboxyisopropylacrylamide) (P(IPAAm-*co*-CIPAAm)) copolymer grafted onto tissue culture grade polystyrene (TCPS) dishes permits RGDS immobilization. These surfaces facilitate the spreading of human umbilical vein endothelial cells (HUVECs) without serum depending on RGDS surface content at 37 °C (above the lower critical solution temperature, LCST, of the copolymer). Moreover, cells spread on RGDS-immobilized surfaces at 37 °C detach spontaneously by lowering culture temperature below the LCST as hydrated grafted copolymer chains dissociate immobilized RGDS from cell integrins. These cell lifting behaviors upon hydration are similar to results using soluble RGDS in culture as a competitive substitution for immobilized ligands. Binding of cell integrins to immobilized RGDS on cell culture substrates can be reversed spontaneously using mild environmental stimulation, such as temperature, without enzymatic or chemical treatment. These findings are important for control of specific interactions between proteins and cells, and subsequent "on−off" regulation of their function. Furthermore, the method allows serum-free cell culture and trypsin-free cell harvest, essentially removing mammalian-sourced components from the culture process.

Introduction

Specific interactions between biomolecules and their molecular recognition play important roles in biology and physiology. Particularly, interactions between cell receptors and bioactive extracellular matrix proteins are necessary to maintain multiple cell functions. Appropriate chemical methodologies for biomaterial design that regulate bioactivities of proteins and cells are increasingly popular.[1−3] Particularly, control of specific interactions between bioactive molecules has been used to study, understand and control molecular recognition mediating biological process.[4,5] Recently, intelligent materials that exploit stimuli-responsive properties have demonstrated "on−off" control of various functional changes useful for biomedical applications.[6−8] Hoffman et al. have conjugated thermally responsive polymers with streptavidin near the biotin binding site to control the binding affinity of biotinylated proteins using a "polymer-shielding" effect.[9] They found that these "affinity switches" attributed to the degree of shielding depended on both the size of the biotinylated protein and the size of the grafted polymer. Moreover, we had previously shown regulation of protein binding to surface-immobilized ligands using the spacer molecules and expanded coil/collapsed changes of co-immobilized temperature-responsive polymers.[10] Chromatographic analyses showed a clear correlation between spacer length and binding capacity by applying step temperature gradients.

The interaction of ligands and cell membrane receptors plays multiple important roles for inducing cell spreading, proliferation, differentiation, and signal transduction.[11−15] The extracellular matrix (ECM) elaborated by cells on surfaces constitutes a regulator of the cell adhesion process, cell differentiation, and contributes to the mechanical properties of tissue. These regulatory effects of ECM are mediated through transmembrane proteins specialized in cell−substrate adhesion. The peptide sequence Arg−Gly−Asp (RGD) found in fibronectin, type I collagen, and other extracellular matrix proteins has been widely studied as an immobilized cell adhesion ligand specific for integrin-mediated cell adhesion.[16,17] Surface density and chemical presentation of these synthetic ligands and their effectiveness as surface modification agents in cell culture is correlated to their ability to enhance cell adhesion, particularly, useful for applications in tissue engineering.[18−25]

In this study, we have designed the "on−off" switching study between cell integrins and the ligand peptide RGDS (Arg−Gly−Asp−Ser) in culture using noninvasive thermal

* To whom the correspondence should be addressed. E-mail: tokano@abmes.twmu.ac.jp. Tel: +81-3-3353-8111 ext. 30233. Fax +81-3-3359-6046.

† Waseda University.

‡ Tokyo Women's Medical University.

10.1021/bm0343601 CCC: $27.50
Published on Web 01/14/2004

control. Temperature responsive poly(*N*-isopropylacrylamide) (PIPAAm)-grafted surfaces are modified with RGDS peptides. Surface swelling, wettabilities, and modulus of the grafted surfaces can be changed by temperature control. Above the lower critical solution temperature (LCST) of PIPAAm, the grafted polymer chains collapse, and the immobilized peptide is therefore exposed to adherent cells. Below the LCST, hydrated polymer chains soften, expand, and swell, shielding immobilized RGDS from integrin access, limiting cell-surface attachment tension, and mechanically disrupting cell-surface contacts. Adherent cell populations are first rounded and then removed under this thermal treatment in the absence of serum proteins or trypsin treatment. The approach obviates the need for exogenous protein addition during culture and is useful for serum-sensitive or trypsin-sensitive cell types, particularly those useful for biomedical tissue engineered devices.

Experimental Section

Materials. *N*-Isopropylacrylamide (IPAAm) was kindly provided from Kojin Co. (Tokyo, Japan), and purified by recrystallization from *n*-hexane. 2-Carboxyisopropylacrylamide (CIPAAm) was synthesized as described previously.[26] Acrylic acid (AAc) was purchased from Wako Pure Chemicals Co., (Tokyo, Japan) and distilled under reduced pressure. Tissue culture grade polystylene (TCPS) dishes (Falcon 3001) were purchased from Becton Dickinson Labware (Oxnard, CA). Both RGDS (−Arg−Gly−Asp−Ser−) and RGES (−Arg−Gly−Glu−Ser−) linear peptides were purchased from Sigma (St. Louis, MO). 1-Ethyl-3-(3-dimethylaminopropyl)-carbodiimide hydrochloride (WSC) was purchased from Dojindo Laboratories (Kumamoto, Japan). Trypsin-EDTA solution, streptomycin, and penicillin were purchased from Gibco BRL (Grand Island, NY). Human umbilical vein endothelial cells (HUVECs), EBM-2 as their medium, and EGM-2 as supplements for medium were purchased from BioWhittaker (Walkersville, MD).

Preparation of Temperature-Responsive Polymer-Grafted Surfaces Modified with Peptides. PIPAAm-grafted surfaces were prepared as described previously.[27,28] Briefly, IPAAm and CIPAAm (used as carboxylate-terminated comonomer for peptide immobilization) were dissolved in 2-propanol at a total concentration of 55% (wt/wt) and 30 μL of the solution is spread uniformly over the surface of 35-mm TCPS dishes. These solutions contained different concentrations of CIPAAm comonomer (1−10 mol %) in the feed. Then, electron beam irradiation using an area beam electron processing system (Curetron EBC-200-AA2, Nissin High Voltage Co. Ltd., Kyoto, Japan) at a radiation dose of 0.3 MGy polymerizes and covalently grafts these monomers onto the TCPS surfaces. After rinsing and drying, 1 mL of Dulbecco's phosphate buffered saline (PBS; pH7.4) containing both RGDS (2 mM) and the same amount of WSC (2 mM) were spread over the surfaces at room temperature. The reacted peptide amount was large excessive to the surface carboxyl group content. Similarly RGES-immobilized surfaces, with the substitution of glutamic acid (E) for aspartic acid (D), were prepared to confirm the biospecificity of the RGDS motif toward HUVEC integrins. Moreover, to compare different presentations of peptides via carboxylic comonomer immobilization, P(IPAAm-*co*-AAc)-grafted surfaces were also prepared and reacted with RGDS by identical methods. After 24 h, these dishes were rinsed with distilled water and sterilized with ethylene oxide after drying. These RGDS and RGES-immobilized P(IPAAm-*co*-CIPAAm)-grafted TCPS surfaces were abbreviated as RGDS−IC(X) and RGES−IC(X), respectively, and RGDS-immobilized P(IPAAm-*co*-AAc)-grafted TCPS surfaces was abbreviated as RGDS−IA(X), where X is the mole percent of carboxylated monomer in feed.

Cell Spreading Assay. HUVECs were cultured on TCPS dishes with EBM-2 supplemented with EGM-2 containing hFGF−B, VEGF, R3IGF-1, ascorbic acid, heparin, hEGF, hydrocortisone, gentamaicin/amphotericin-B (GA-1000) and fetal bovine serum (FBS) in humidified atmosphere with 5% CO_2. The cells were harvested from TCPS dishes with 0.25% trypsin−0.26 mM EDTA in phosphate buffered saline (PBS). Subcultures up to passage 3 were used for this study. EBM-2 supplemented with EGM-2 except for FBS was added, and the cells were centrifuged and resuspended in the serum-containing (2% FBS) or serum-free medium. A fixed number of cells (1.0×10^5 cells in 1 mL serum-free culture medium) were plated onto RGDS-immobilized PIPAAm-grafted surfaces and cultured in serum-free media at 37 °C in humidified atmosphere, 5% CO_2. Cell morphology was monitored and photographed under a phase contrast microscope (TE300, Nikon, Tokyo) after 6- and 24-h culture. In this study, "spread cell" are defined as well-adherent flat-shaped cell. The cell number was also counted from printed photographs and presented as mean ± standard deviation ($n = 3$).

Cell Detachment Assay. The lifting behavior of HUVECs from RGDS−IC(X) was investigated both by low-temperature treatment and soluble RGDS addition after indicated culture times without serum at 37 °C (4 h, 1 day, 3 days, and 7 days). For low-temperature treatment, spread cells were transferred to a CO_2 incubator equipped with a cooling unit fixed at 20 °C. For the competitive assay, soluble RGDS (100 μM) was added into culture dishes and incubated at 20 and 37 °C. The cell morphology was continuously observed and microphotographed under a phase contrast microscope. The percentage of spread cells to the initial spread cells was presented as a mean ± standard deviation ($n = 3$).

Results

Enhancement of Cell Spreading Mediated by Biospecific Interaction between Cell Integrins and Immobilized RGDS. To confirm the biospecificity of RGDS immobilized on grafted temperature-responsive polymers, HUVECs were seeded onto RGDS−IC(X) under serum-free conditions at 37 °C. The spread cell number after a 6-h culture increased depending on the co-monomer carboxylate group density on the surface, resulting from increasing RGDS immobilization probability to carboxyl groups on these surfaces (Figure 1).

Immobilized RGDS contributed to enhancement of cell spreading, likely mediated by cell integrins. By contrast, the control RGES-immobilized surfaces (RGES−IC(X)) did not

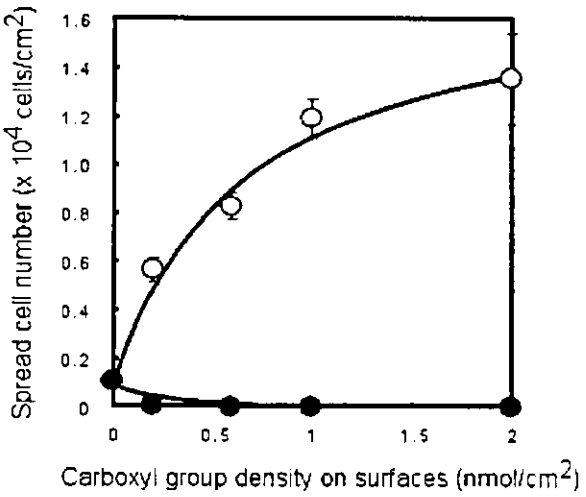

Figure 1. HUVEC spreading on RGDS and RGES-immobilized temperature-responsive culture surfaces after a 6-h culture without serum at 37 °C. These peptides were covalently grafted on P(IPAAm-*co*-CIPAAm)-grafted surfaces. The feed concentration of peptides was 2 mM. Symbols: RGDS−IC(X) (open circle) and RGES−IC(X) (closed circle).

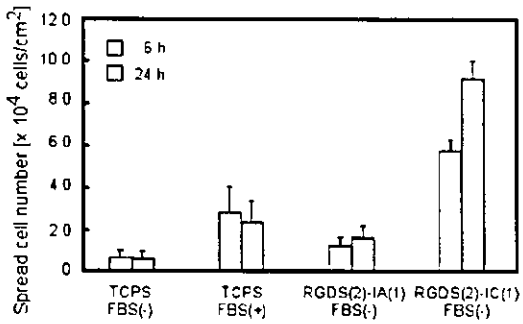

Figure 2. Comparisons of HUVEC spreading on various culture surfaces after 6- or 24-h cultures with or without serum at 37 °C. The surfaces used in this experiment were TCPS with/without serum, RGDS−IA(1) without serum, and RGDS−IC(1) without serum.

demonstrate cell spreading enhancement against immobilized peptides density because they have no integrin biospecificity with the substitution of glutamic acid (E) for aspartic acid (D).[29] Figure 2 shows spread HUVEC numbers on various substrates after 6-h and 24-h cultures with or without serum at 37 °C. Although addition of dilute serum facilitates HUVEC spreading on TCPS, RGDS−IC(1) promoted cell spreading dramatically under serum-free conditions. By contrast, spreading improvement was hardly observed on the RGDS−IA(1) surface where peptides are immobilized via another comonomer, AAc, in place of CIPAAm. As seen in Figure 3, significant differences in HUVEC spreading on P(IPAAm-*co*-CIPAAm)-grafted surfaces (CIPAAm; 1 mol % in feed) before and after RGDS immobilization after a 6-h culture without serum at 37 °C are readily evident.

Dissociation Control of Integrin−RGDS Specific Interactions. To control dissociation of specific interactions between cultured cell integrins and surface RGDS, spread HUVECs (1 day culture without serum at 37 °C) were exposed to the addition of soluble RGDS at 37 °C (Figure 4) and lower temperature treatment at 20 °C (Figure 5). Soluble RGDS (100 μM) spontaneously detaches HUVECs from RGDS−IC(X) based on competitive substitution of

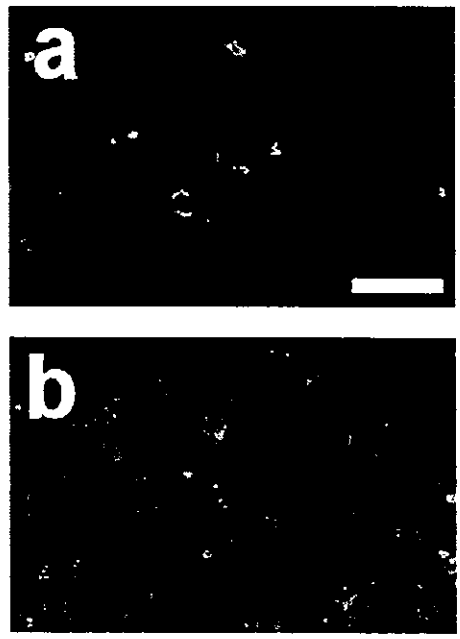

Figure 3. Phase-contrast photographs of HUVECs on temperature-responsive culture surfaces after a 6-h culture without serum at 37 °C before (a) and after (b) 2 mM of RGDS surface immobilization. Bar = 100 μm.

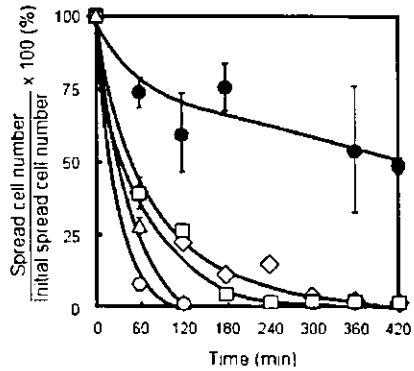

Figure 4. Competitive assay for HUVEC detachment from RGDS-immobilized temperature-responsive culture surfaces by soluble peptide addition. Soluble RGDS (100 μM) was added to cells on RGDS−IC(X) after a 24-h culture at 37 °C without serum. CIPAAm compositions were 1 (open circle), 3 (triangle), 5 (square), and 10 mol % (diamond). As a comparison, cells cultured on TCPS for 24 h at 37 °C with serum were detached at 20 °C (closed circle).

soluble RGDS for immobilized RGDS. Detachment rates depended on immobilized cell adhesive peptide densities represented by monomer carboxylate group composition in each feed. Moreover, detachment rates were accelerated dramatically by addition of higher concentrations of RGDS (data not shown). Low-temperature treatment at 20 °C also promoted cell detachment from RGDS−IC(X), where the detachment rate also decreased with increasing cell adhesive peptide surface content. Both treatments (addition of soluble RGDS at 20 °C) together accelerated cell detachment from RGDS−IC(5) over each separately (Figure 6).

To examine time-dependent cell-substrate interactions, HUVECs were cultured on RGDS−IC(1) for 4 h, 1 day, 3 days, and 7 days without serum at 37 °C and subjected to either addition or nonaddition of soluble RGDS at 37 or 20

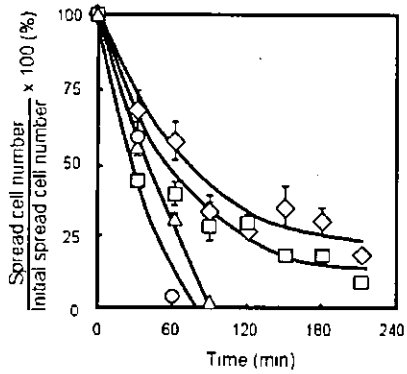

Figure 5. HUVEC detachment from RGDS-immobilized temperature-responsive culture surfaces by lowering the temperature. Cells on RGDS−IC(X) were subjected to low-temperature treatment at 20 °C after a 24-h culture at 37 °C without serum. CIPAAm compositions were 1 (open circle), 3 (triangle), 5 (square), and 10 mol % (diamond).

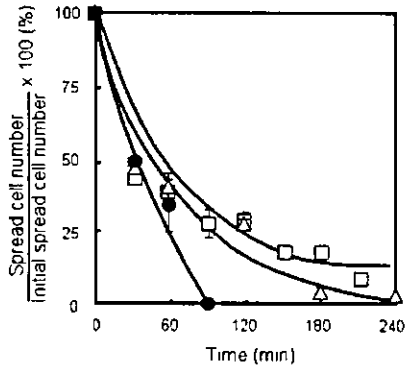

Figure 6. Comparison of the effects of soluble peptide addition and reduced culture temperature treatment on HUVEC detachment from RGDS−IC(5). Soluble RGDS (100 μM) was added into each culture dish after 24-h culture at 37 °C without serum, and these surfaces were incubated at 20 and 37 °C. Soluble RGDS (100 μM) addition (triangle), only temperature treatment at 20 °C (square), and temperature treatment at 20 °C with 100 μM of soluble RGDS (closed circle).

°C (Figure 7). Soluble RGDS addition became less effective with increasing culture time before each treatment (Figure 7a). With lower temperature treatment, detachment rates increased with increasing culture time (Figure 7b). Moreover, both treatments accelerated cell detachment from RGDS−IC(1), particularly after 1 and 3 day cultures (Figure 7c).

Discussion

Cell integrin ligand RGDS peptides covalently immobilized to temperature-responsive polymer grafted surfaces were assayed for cell attachment/detachment "on−off" control by culture temperature regulations. Polymer grafted amounts on the surface are approximately 2 μg/cm^2 estimated by attenuated total reflection Fourier transform infrared (ATR-FTIR) as described previously.[28] Carboxylate group densities on these surfaces calculated from the feed composition of CIPAAm were 0.2, 0.6, 1.0, and 2.0 nmol/cm^2 for RGDS(X)-IC(1), IC(3), IC(5), and IC(10), respectively. Hydrated shielding abilities of the polymers against ligands would depend on the relative size of the polymer chains to receptor active binding sites.[9] Changes in surface hydration,

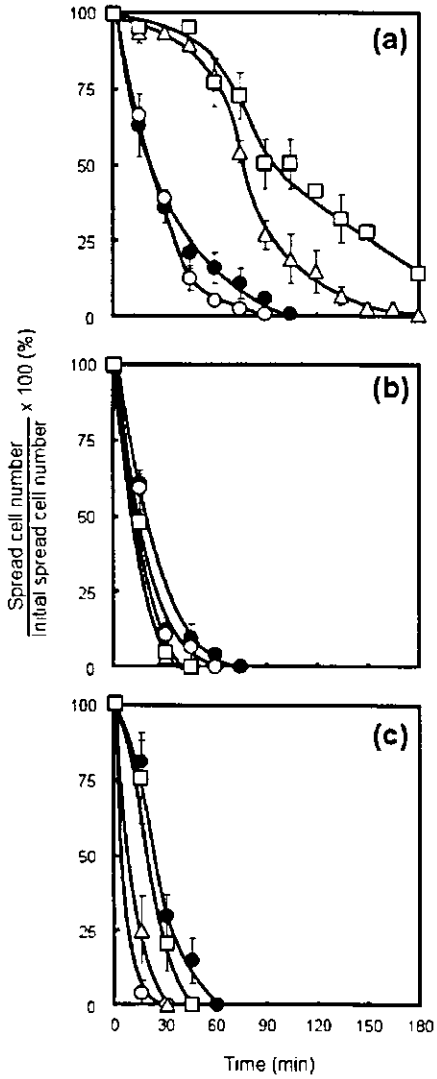

Figure 7. Effect of culture time of HUVECs on cell-substrate interaction. Cells seeded onto RGDS−IC(1) were cultured at 37 °C for 4 h (closed circle), 1 day (open circle), 3 day (triangle), and 7 days (square) and subjected to the following treatments: Soluble RGDS (100 μM) addition (a), only temperature treatment at 20 °C (b), and temperature treatment at 20 °C with 100 μM of soluble RGDS (c).

surface mechanical modulus, and support of spread cells in tension ("tensegrity")[30−34] would also depend on surface graft architecture, swelling below LCST, and less surface structural rigidity.

As seen in Figures 1−3, immobilization of RGDS on surfaces was critical for HUVEC spreading at 37 °C. RGDS enhanced integrin-mediated cell spreading, whereas the control tetrapeptide (RGES) did not (Figure 1), indicating recognition specificity. Healy et al. also showed that few or no focal contacts were formed by bone-derived cells on the RGE-immobilized surfaces and there was a significant difference between the adhesion strength of cells to RGD and RGE-immobilized surfaces.[35] Moreover, scant cell spreading was also observed for surfaces grafted with comonomer, AAc, in place of CIPAAm (Figure 2). Copolymerization of IPAAm with AAc shifts its LCST to a temperature higher than 37 °C,[36−38] and we have already

reported that P(IPAAm-*co*-CIPAAm) retains PIPAAm's thermal phase transition behavior because CIPAAm maintains a hydration environment around side chain groups essential to the phase transition.[26,39] We conclude, therefore, that low cell spreading on RGDS−IA(1) is attributed to highly hydrated, unreacted acrylic acid carboxyl groups distinct from CIPAAm surfaces.

HUVEC detachment behavior from RGD-IC(X) by reducing the temperature below the polymer LCST depended upon the immobilized RGDS content (Figure 5). This behavior was very analogous to that produced by soluble RGDS addition (Figure 4). Although HUVECs cultured in FBS on TCPS resisted detachment by soluble RGDS addition, all spread cells detached from RGDS−IC(X) consistent with respective immobilized RGDS amounts. This mechanism is explained by competitive ligand−receptor binding affinity changes, where substitution of the soluble RGDS ligand for immobilized RGDS occurs readily on lower peptide density surfaces such as RGDS−IC(1). HUVEC detachment by reducing the temperature is also explained by a decreasing association between cell integrins and the RGDS by surface swelling and loss of cell tension on hydrated polymer grafted chains. It is not likely that low temperature treatment directly causes integrin-RGDS dissociation because it is well-known that cell−matrix binding is retained even at 4 °C.[40] Mrksich et al. pointed out that available ligand densities for binding cellular receptors depended on ligand conditions because the adsorbed ligand distribution, conformation, and orientation were changed by the choice of substrates.[41] It is plausible that only slight microenvironmental changes of immobilized ligands caused by temperature-dependent swelling of ligand-attached polymer chains reduces surface rigidity upon which adherent cells are attached. Because these spread cells are in tension, a sudden loss of this tension and traction prompts detachment and rounding. Cell receptor−ligand occupancy is a function of surface cell spreading and tension: when hydrated and softened, the polymers promote ligand−receptor dissociation. This result is similar to the competitive detachment assay by soluble RGDS addition. Accelerated cell detachment behavior in Figure 6 suggests possible additivity of soluble RGDS addition and low temperature treatment that drastically dissociate the receptor from the ligand.

The cell−substrate interaction occurs in a series of steps beginning with sufficient minimal integrin-mediated binding, followed by increasing receptor recruitment, cell polarization, and cytoskeletal and cytoplasmic reorganization.[42] Cells alter the formation of adhesive contacts with the substrate, including receptor clusters and focal contact adhesion, in a time-dependent manner.[43,44] Therefore, we propose that HUVECs change their interactions with RGDS−IC(X) as a function of culture time before cell detachment assay. Large differences in the effects of soluble RGDS addition on cell detachment are observed between 1 day and 3 day cultures at 37 °C (Figure 7a). Delayed cell detachment after a 3 day (or 7 day) culture is attributed to additional interactions developing between cells and surfaces including extracellular matrix production, remodeling, and nonspecific interactions. Hence, with increasing time, cells resist surface removal even if the specific, original integrin-mediated ligand interactions dissociate. Although slower with culture time, all cells detach eventually because loss of cell tension by the dissociation of integrin-RGDS binding likely triggers several signal transduction mechanisms for cytoskeletal changes, rounding, and dissociation of other interactions with the substrate. In contrast, the detachment rates of cells by reducing the temperature increases with increasing culture time because long-term culture increases nonspecific cell−surface interactions (lower affinity than specific integrin−RGDS interactions) but are all induced to release by grafted polymer swelling surface softening and low cell tension on the surface (Figure 7b). Both treatments (lowering the temperature and soluble RGDS addition) resulted in acceleration of cell detachment, but degrees of acceleration were slight because in this system low temperature treatments more effectively produce cell detachment compared with soluble RGDS addition at this concentration (100 μM).

In conclusion, RGDS-immobilized temperature-responsive polymer-grafted surfaces promote the HUVEC adhesion and spreading by their biospecific activity in serum-free media. At temperatures below the grafted polymer's LCST, integrin−RGDS association decreases due to loss of cell tension and surface anchoring, prompting cells to round and then detach. Observed "on−off" control of specific integrin-RGDS binding only by temperature regulation is very important for cell function regulation because cell surface integrins not only bind to cell adhesive ligands in ECM but also serve to produce subsequent cell signal transduction activity. Moreover, this approach facilitates a serum-free cell culture for the safety of clinical applications using cultured cells and noninvasive cell recovery (no enzymes) that help maintaining original cell function, both important to applications of tissue engineering.

Acknowledgment. We appreciate the continued useful comments and technical criticisms from Prof. D. W. Grainger (Colorado State University, CO). This work is supported in part by Grants-in-Aid for Scientific Research by Ministry of Education, Culture, Sports, Science and Technology of Japan. The present study is supported in part by Japan Ministry for Culture, Sports, Education, Science and Technology, Core Research for Evolutional Science and Technology (CREST).

References and Notes

(1) Whitesides, G. M.; Mathias, J. P.; Seto, C. T. *Science* **1991**, *254*, 1312−1319.
(2) Irvine, D. J.; Mayes, A. M.; Griffith, L. G. *Biomacromolecules* **2001**, *2*, 85−94.
(3) Yamato, M.; Kwon, O. H.; Hirose, M.; Kikuchi, A.; Okano, T. *J. Biomed. Mater. Res. Short Commun.* **2001**, *55*, 137−140.
(4) Fong, R. B.; Ding, Z.; Long, C. J.; Hoffman, A. S.; Stayton, P. S. *Bioconjugate Chem.* **1999**, *10*, 720−725.
(5) Schlosser, M.; Hahmann, J.; Ziegler, B.; Augstein, P.; Ziegler, M. *J. Immunoassay* **1997**, *18*, 289−307.
(6) Kumar, A.; Kamihira, M.; Galaev, I. Y.; Mattiasson, B.; Iijima, S. *Biotechnol. Bioeng.* **2001**, *75*, 570−580.
(7) Tang, A.; Wang, C.; Stewart, R. J.; Kopecek, J. *J. Controlled Release* **2001**, *72*, 57−70.
(8) Kurisawa, M.; Yokoyama, M.; Okano, T. *J. Controlled Release* **2000**, *69*, 127−137.
(9) Ding, Z.; Fong, R. B.; Long, C. J.; Stayton, P. S.; Hoffman, A. S. *Nature* **2001**, *411*, 59−62.

(10) Yoshizako, M.; Akiyama, Y.; Yamanaka, H.; Shinohara, Y.; Hasegawa, Y.; Carredano, Enrique.; Kikuchi, A.; Okano, T. *Anal. Chem.* **2002**, *74*, 4160−4166.
(11) Hynes, R. O. *Cell* **1992**, *69*, 11−25.
(12) Miyamoto, S.; Akiyama, S. K.; Yamada, K. M. *Science* **1995**, *267*, 883−885.
(13) Chicurel, M. E.; Chen, C. S.; Ingber, D. E. *Curr. Opin. Cell Biol.* **1998**, *10*, 232−239.
(14) Grinnell, F. *Trends Cell Biol.* **2000**, *10*, 362−365.
(15) Grinnell, F. *Int. Rev. Cytol.* **1978**, *53*, 65−144.
(16) Piershbacher M. D.; Rouslahti E. *Proc. Natl. Acad. Sci. U.S.A.* **1984**, *81*, 5985−5988.
(17) Yamada, K. M. *J. Biol. Chem.* **1991**, *266*, 12809−12812.
(18) Massia, S.; Hubbell, J. A. *J. Cell. Biol.* **1991**, *114*, 1089−1100.
(19) Houseman, B. T.; Mrksich, M. *Biomaterials* **2001**, *22*, 943−955.
(20) Maheshwari, G.; Brown, G.; Lauffenburger, D. A.; Wells, A.; Griffith, L. G. *J. Cell Sci.* **2000**, *113*, 1677−1686.
(21) Stile, R. A.; Healy, K. E. *Biomacromolecules* **2001**, *2*, 185−194.
(22) Rezania, A.; Healy, K. E. *J. Biomed. Mater. Res.* **2000**, *52*, 595−600.
(23) Garcia, A. J.; Keselowsky, B. G. *Crit. Rev. Eukaryot. Gene Expr.* **2002**, *52*, 151−162.
(24) Saneinejad, S.; Shoichet, M. S. *J. Biomed. Mater. Res.* **1998**, *42*, 13−19.
(25) Tong, Y. W.; Shoichet, M. S. *J. Biomater. Sci. Polym. Ed.* **1998**, *9*, 713−729.
(26) Aoyagi, T.; Ebara, M.; Sakai, K.; Sakurai, Y.; Okano, T. *J. Biomater. Sci. Polym. Ed.* **2000**, *11*, 101−110.
(27) Kikuchi, A.; Okuhara, M.; Karikusa, F.; Sakurai.; Okano, T. *J. Biomater. Sci. Polym. Ed.* **1998**, *9*, 1331−1348.
(28) Ebara M.; Yamato, M.; Hirose, M.; Aoyagi T.; Sakai K.; Okano T. *Biomacromolecules* **2003**, *4*, 344−349.
(29) Hautanen, A.; Gailit, J.; Mann, D. M.; Ruoslahti, E. *J. Biol. Chem.* **1989**, *264*, 1437−1442.
(30) Chicurel, M. E.; Chen, C. S.; Ingber, D. E. *Curr. Opin. Cell Biol.* **1998**, *10*, 232−239.
(31) Ingber, D. E. *Annu. Rev. Physiol.* **1997**, *59*, 575−599.
(32) Ingber, D. E.; Dike, L.; Hansen, L.; Karp, S.; Liley, H.; Maniotis, A.; McNamee, H.; Mooney, D.; Plopper, G.; Sims, J. *Int. Rev. Cytol.* **1994**, *150*, 173−224.
(33) Ingber, D. E. *Cell* **1993**, *75*, 1249−1252.
(34) Ingber, D. E. *J. Cell Sci.* **1993**, *104*, 613−27.
(35) Rezania, A.; Thomas, C. H.; Branger, A. B.; Waters, C. M.; Healy, K. E. *J. Biomed. Mater. Res.* **1997**, *37*, 9−19.
(36) Feil, H.; Bae, Y. H.; Feijen, J.; Kim, S. W. *Macromolecules* **1993**, *26*, 2496−2500.
(37) Kaneko, Y.; Nakamura, S.; Sakai, K.; Aoyagi, T.; Kikuchi, A.; Sakurai, Y.; Okano, T. *Macromolecules* **1998**, *31*, 6099−6105.
(38) Yu, H.; Grainger, D. W. *J. Appl. Polym. Sci.* **1993**, *49*, 1553−1563.
(39) Ebara, M.; Aoyagi, T.; Sakai, K.; Okano, T. *Macromolecules* **2000**, *33*, 8312−8316.
(40) Grinnell, F.; Lang, B. S. *J. Cell. Biol.* **1981**, *87*, p127a.
(41) Mrksich, M. *Chem. Soc. Rev.* **2000**, *29*, 267−273.
(42) Benjamin, G.; Bershadsky, A.; Pankov, R.; Yamada, K. M. *Nat. Rev.* **2001**, *2*, 793−805.
(43) Baneyx, G.; Baugh, L.; Vogel, V. *Proc. Natl. Acad. Sci. U.S.A.* **2002**, *99*, 5139−5143.
(44) Dejana, E.; Colella, S.; Conforti, G.; Abbadini, M.; Gaboli, M.; Marchisio, P. C. *J. Cell. Biol.* **1988**, *107*, 1215−1223.

BM0343601

Scientific Discovery

Most of the papers in this section are studies of cellular biology in urological cancer. Each of the four papers assess a particular aspect of four different types of cancer: prostate, bladder, renal, and testicular. The other two reports are on unrelated issues; in the first, the authors write about urothelial regeneration using viable cultured urothelial cell sheets grafted onto demucosalized gastric flaps, and in the second, on the *in vivo* expression of nitric oxide synthase.

Urothelium regeneration using viable cultured urothelial cell sheets grafted on demucosalized gastric flaps

Y. SHIROYANAGI*†, M. YAMATO*‡, Y. YAMAZAKI†, H. TOMA† and T. OKANO*‡
Institute of Advanced Biomedical Engineering and Science and †Department of Urology, Tokyo Women's Medical University, and ‡CREST, Japan Science and Technology Corporation, Tokyo, Japan

Accepted for publication 7 January 2004

OBJECTIVE

To evaluate urothelium regeneration by grafting viable cultured urothelial cell sheets, harvested from temperature-responsive culture surfaces, on demucosalized gastric flaps in a dog model.

MATERIALS AND METHODS

Viable urothelium was obtained from eight beagle dogs by partial cystectomy. Harvested urothelial cells were seeded on temperature-responsive culture dishes modified with the thermally sensitive polymer, poly(N-isopropylacrylamide). Urothelial cells cultured for 3 weeks generated contiguous urothelial cell sheets that were noninvasively harvested with no enzymatic treatment from these dishes, by reducing culture temperature. Urothelial cell sheets were autografted onto surgically demucosalized gastric flaps. Three weeks after autografting the dogs were killed and the gastric flaps with the urothelial cell sheets were examined. Cell and tissue characteristics were compared between these urothelial cell sheet-grafted gastric flaps and native urothelium. Ultrafine structures were also examined by electron microscopy.

RESULTS

Five of the eight urothelial cell sheet-grafted flaps showed viable urothelial regeneration. Urothelial cell sheets attached spontaneously to demucosalized tissue surfaces completely, with no suture or fixing, and developed into a stratified viable epithelium very similar to native urothelium. Regenerated urothelium remained unstained by antiproton pump antibody, which typically stains epithelial cells positively in gastric mucosal layers. On three of the eight flaps where there were severe haematomas, grafted cell sheets were not adherent and there was no urothelial regeneration.

CONCLUSIONS

Urothelial cell sheets were autografted onto dog demucosalized gastric flaps successfully, with no suture or fixation, generating a multilayered urothelium *in vivo*. The novel intact cell-sheet grafting method rapidly produces native-like epithelium *in vivo*. This versatile technology should prove useful in urinary tract tissue engineering and surgical reconstruction.

KEYWORDS

urothelium, cell sheet engineering, temperature-responsive culture surfaces, autologous transplantation, bladder augmentation, tissue regeneration

INTRODUCTION

Bladder reconstruction has an increasingly important role in the treatment of adult and paediatric patients after bladder resection for malignancy, or with low-compliance, low-capacity bladders. The indications for urinary diversion and reconstruction using intestinal segments have expanded greatly. However, gastrointestinal mucosa often causes various complications, including electrolyte imbalance, stone formation, UTI and mucus production [1,2]. To solve these complications some investigators have attempted to cover the demucosalized intestinal surface with urothelial grafts obtained from the bladder mucosa or cultured urothelium [3–5].

Previous work in our laboratory showed that various intact cell sheets from diverse primary sources, including urothelium, can be harvested intact with no enzymatic proteolysis (e.g. trypsin or dispase digestion), by using temperature-responsive culture systems [6–8]. In the present study native gastrointestinal mucosa was replaced with cultured urothelial cell sheets harvested noninvasively from temperature-responsive culture surfaces in a surgical dog model of reconstruction. The purposes of this study were; (i) to investigate the utility of direct grafting of cultured urothelial cell sheets transplanted onto demucosalized gastric flaps, and (ii) to examine the histology of urothelial regeneration on the gastrointestinal stromal layer.

MATERIALS AND METHODS

All experimental protocols were approved by the animal welfare committee of Tokyo Women's Medical University (Approval no. 02-55, 2002). The experimental scheme is shown in Fig. 1; nine dogs underwent the procedures under general anaesthesia. Eight adult beagle dogs (10–12 kg, 1 year old, female) first had a partial cystectomy to obtain urothelial cells, and these primary urothelial cells were seeded on temperature-responsive culture dishes. Three weeks later the same dogs were re-anaesthetized and a segment of stomach isolated and demucosalized. Cultured urothelial cell sheets were autografted onto exposed gastric submucosal layers of surgically constructed flaps by simple topical placement with no sutures or fixation, but the flap was placed within a protective latex pouch to prevent abdominal adhesion, and returned to the abdominal cavity. After a further 3 weeks all dogs were killed and the transplanted flaps excised and examined. In one dog (a control) no cell sheet was grafted during identical surgery.

FIG. 1. Scheme for the urothelial cell sheet autografting experiment. Canine urothelial cells were isolated and cultured on temperature-responsive culture dishes. The urothelial cell sheets, noninvasively harvested by reducing culture temperature after 3 weeks, were autografted onto a canine demucosalized gastric flap surgical model.

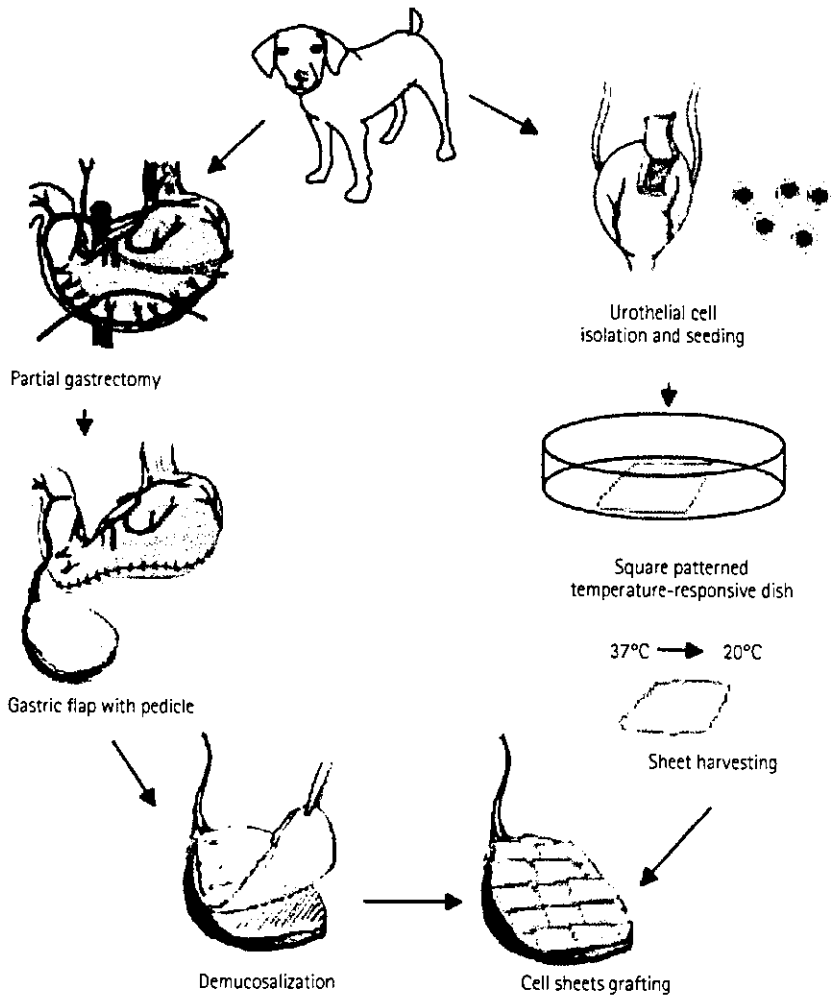

For anaesthesia the dogs were premedicated with 0.04 mg/kg atropine and 15 mg/kg ketamine intramuscularly, and then given 15 mg/kg thiopental sodium. An endotracheal tube was then placed and anaesthesia maintained using halothane and nitrous oxide.

For urothelial cell sheet preparation, a laparotomy was made via midline incision and a 2.0 × 2.0 cm area was excised from the dome of the bladder. The bladder was closed in one layer. Both urothelium and submucosal layers were stripped from the smooth muscle layer and treated with 1000 U/mL dispase (Godoshusei, Tokyo, Japan). After this enzymatic treatment the epithelial layer was peeled from the stromal layer and digested in 0.1% trypsin/0.04% EDTA to obtain a single-cell suspension. Then 1–2 $\times 10^5/cm^2$ dissociated urothelial cells were seeded onto square-patterned temperature-responsive cultured dishes and cultured according to the method of Rheinwald and Green [9,10] with a feeder layer of mitomycin C-treated NIH 3T3 cells. The culture medium was Ham's F-12 medium/DMEM in a 1 : 3 ratio supplemented

FIG. 2. Urothelial cell sheets and demucosalized gastric flaps. Macroscopic view of square-patterned urothelial cell sheets harvested by reducing culture temperature. Without substrate support, the sheet will respond to internal cell stresses to deform plastically over time after release, (a). H&E staining of the urothelial cell sheet shows multilayers of cultured urothelial cells in sheets, (b). Anti-uroplakin antibody staining along the apical surface of the urothelial cell sheets, (c). Macroscopic view of the demucosalized gastric flaps, (d). Scale bar represents 1 cm in (a) and (d), and 100 μm in (b) and (c), respectively.

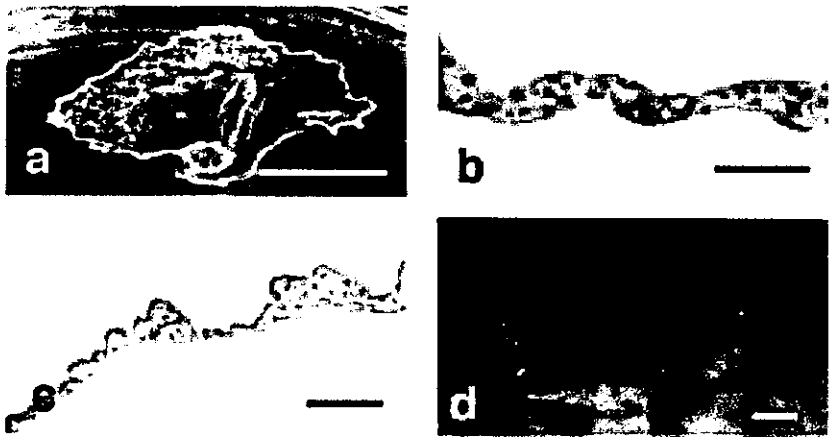

with 5% fetal bovine serum, insulin (5.0 μg/mL), transferrin (5.0 μg/mL), triiodothironine (2 nmol/L), cholera toxin (1 nmol/L), hydrocortisone (0.4 μg/mL), recombinant human epidermal growth factor (Gibco BRL Life Technologies, Grand Island, NY, 10 ng/mL), recombinant fibroblast growth factor-7 (R&D Systems, Inc., Minneapolis, MN, 10 ng/mL), penicillin and streptomycin. Three weeks later the dishes were incubated at 20 °C for 30 min to yield contiguous, intact urothelial cell sheets free from the culture substrate, floating in media (Fig. 2a). These sheets were transferred immediately *in vivo* to tissue surfaces.

For the autografts of urothelial cell sheets onto demucosalized gastric flaps, 3 weeks after initial bladder excision the same eight dogs were re-anaesthetized. Through a midline incision a 5–7 cm segment of the greater curvature of stomach was isolated using a Proximate Linear Cutter™ (Ethicon Endo-Surgery, Cincinnati, OH), leaving the gastric segment with its vascular pedicle intact. The mucosa of the isolated gastric segment was then mechanically stripped off with scissors. The surface of the demucosalized gastric flap was cauterized for haemostasis. Urothelial cell sheets harvested from the culture dishes were carefully removed from the dishes and then placed topically directly onto demucosalized gastric flap areas with no fixation. The urothelial cell sheets were transferred with a small transparency sheet because they were too fragile to manipulate with forceps. The flap was then placed in a latex pouch to prevent adhesion and returned to the abdominal cavity.

Standard tissue sections were examined after haematoxylin and eosin (H&E) staining and periodic acid/Schiff reaction. For immunohistochemistry the sections were pretreated with proteinase K (Dako, Denmark), washed in Dulbecco's PBS and blocked with 1% BSA solution. The sections were then incubated with diluted primary antibodies; mouse monoclonal antihuman cytokeratin, AE1/AE3 (Dako), mouse monoclonal antihuman cytokeratin 7, OV-TL 12/30 (Dako), and rabbit antiserum to total bovine uroplakins (kindly provided by Dr T.T. Sun, New York University, NY), rinsed with PBS, and incubated with horseradish peroxidase-conjugated secondary antibody (LASB kit, Dako). Sections were developed with diaminobenzidine and counterstained with haematoxylin. Frozen tissue sections of the grafts were cut at 10 μm, mounted on glass slides and fixed at room temperature with 4% paraformaldehyde in PBS for 20 min. They were then washed with PBS, permeabilized with 0.5% Triton X-100 in PBS for 5 min, washed three times with PBS, and blocked with 0.1% BSA in PBS for 2 h. Primary antibodies used were antiheparan sulphate proteoglycans, A7L6 (Chemicon International, CA, USA), rabbit polyclonal antihuman placental type IV collagen, 10760 (Progen Biotechnik, Heidelberg, Germany) and antiproton pump, 1H9 (Medical & Biological Laboratories, Nagoya, Japan). Sections were incubated with the primary antibodies for 24 h, rinsed with PBS three times and incubated for 2 h with the secondary fluorescein isothiocyanate-conjugated goat anti-IgG antibody (Cappel Products, Aurora, OH, USA).

For electron microscopy, tissue samples were embedded in Quetal 812 (Nisshin, Tokyo, Japan) and ultrathin sections (90 nm) were cut on an ultramicrotome, and then stained with uranyl acetate and lead citrate. The sections were examined at 80 kV using a transmission electron microscope. Other samples were cut into small pieces, fixed in 2.5% glutaraldehyde for 1 h, postfixed in 1.5% osmium tetroxide, dehydrated through graded alcohols, dried with the *t*-butyl alcohol method and osmium-sputtered for 15 s [11]. These samples were examined using a scanning electron microscope.

RESULTS

Square urothelial cell sheets were reliably obtained (Fig. 2a), and consisted of one to four cell layers (Fig. 2b), staining positively with antiuroplakin antibodies (Fig. 2c). The haemorrhage of the demucosalized gastric flap surface was controlled and a thin fibrin layer was found on the surface (Fig. 2d).

None of the nine dogs that underwent surgery died afterward. All demucosalized gastric flaps with and with no cell sheet treatment appeared to be smaller and thicker than the originals at death. There was no gastric mucosal re-growth in the control dog (Fig. 3a). Of the eight dogs with a urothelial cell sheet autograft, five had viable regenerated epithelium (Fig. 3f–j); there was urothelial regeneration on almost all the surface of the grafted gastric flaps. Urothelial cells migrated and covered the small gaps between grafted cell sheets. The morphological structures of the regenerated epithelium on the demucosalized gastric flaps were very similar to native urothelium (Fig. 3b–e), except for the superficial cell layer. There was a squamous change in the superficial layer, and neither gland nor mucous granule morphology in any site of the

FIG. 3. Histological characterization. Control demucosalized gastric graft (noncell sheet treated), (a). Native urothelium of canine ureter, (b–e). regenerated urothelium on a demucosalized gastric flap, (f–j). H&E staining (a,b,f). Periodic acid/Schiff reaction showed no observable mucous granules, (g). There was no gastric mucosal re-growth on the control graft, (a). Regenerated urothelium expresses pan-cytokeratin similarly to that observed for native urothelium, (c,h). The expression of cytokeratin 7 is strong in native urothelium and weak in the regenerated urothelium, (d,i). The regenerated urothelium does not express uroplakin but it is well-expressed in native urothelium, (e,j). Scale bar represents 100 μm.

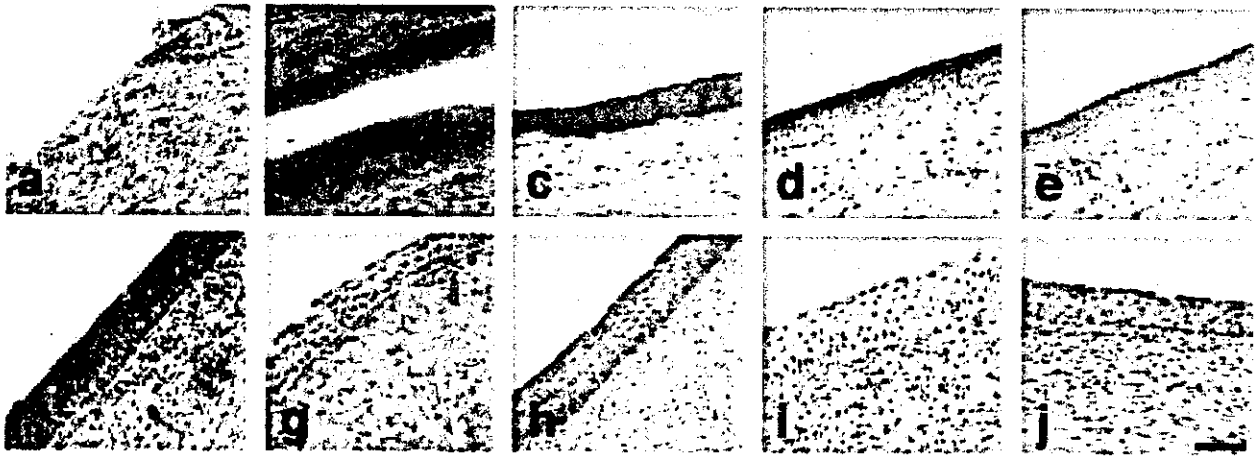

regenerated urothelium (Fig. 3g). Subepithelial tissue was moderately infiltrated with mononuclear cells and showed substantial neovascularization. Urothelium was not regenerated on three of eight flaps where there were severe haematomas.

All layers of regenerated urothelium stained positively with anticytokeratin antibody, similarly to native urothelium (Fig. 3c,h). Cytokeratin 7 was well-expressed in superficial and intermediate cell layers of native urothelium (Fig. 3d), but stained only faintly in regenerated epithelium (Fig. 3i). Uroplakins were strongly expressed in the superficial umbrella cells of native urothelium (Fig. 3e), but were not present in regenerated epithelium (Fig. 3j).

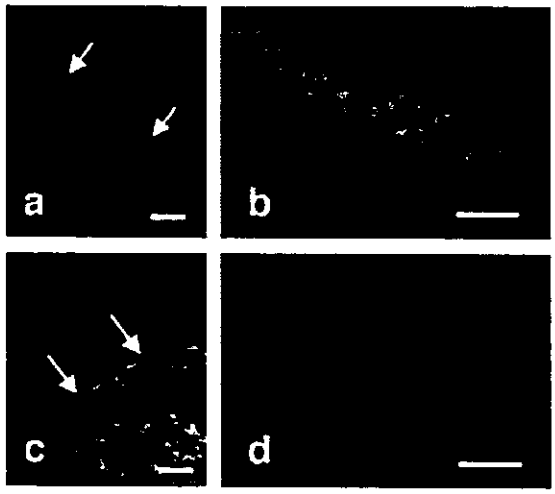

FIG. 4. Immunofluorescence microscopy. The basement membrane (arrow) is positively stained with antiheparan sulphate proteoglycan antibody in native urothelium (a) and in regenerated urothelium (c). The basement membrane of blood vessels was also stained. Note the considerable evidence for revascularization in gastric flaps with regenerated epithelium (c). The proton pump was well-expressed in gastric glands (b), but not in regenerated epithelium (d). Scale bar represents 100 μm.

Heparan sulphate proteoglycan, a typical component of basement membrane, was deposited along the border between regenerated epithelial cell layers and gastric submucosal layers (Fig. 4c), as well as the basal side of the native urothelium (Fig. 4a). Basement membrane from blood vessels was also stained with antibody in both native bladder and gastric flaps with regenerated epithelium. There was more vascularization in the submucosal layer with regenerated epithelium than in the native gastric submucosal layer (data not shown). Basement membrane in regenerated urothelium was also stained with anticollagen IV antibody, similarly to native urothelium (data not shown). Proton pump (H^+, K^+-ATPase), essential to produce gastric acid, was well-expressed in native gastric mucosa (Fig. 4b), but was not in regenerated epithelium (Fig. 4d).

Transmission electron microscopy showed that superficial cells of native urothelium contained numerous cytoplasmic vesicles (Fig. 5a). However, those of the regenerated epithelium had fewer cytoplasmic vesicles and abundant microfilaments (Fig. 5c). Scanning electron microscopy showed the 'cobble-stone' appearance characteristic of native urothelium (Fig. 5b) in the regenerated epithelium (Fig. 5d). However, in regenerated epithelium, the apical cells were smaller than those of native urothelium. Furthermore, native apical cells were flat with tightly connected cell-to-cell borders (Fig. 5b). In contrast, the regenerated apical cells were slightly rounded and each cell appeared isolated (Fig. 5d).

DISCUSSION

In the last decade, many procedures have been examined to solve the complications of

FIG. 5. Scanning and transmission electron microscopy. Native urothelium (a, b) and regenerated urothelium (c, d). (a) and (c) are transmission and (b) and (d) are scanning. Scale bar represents 10 μm.

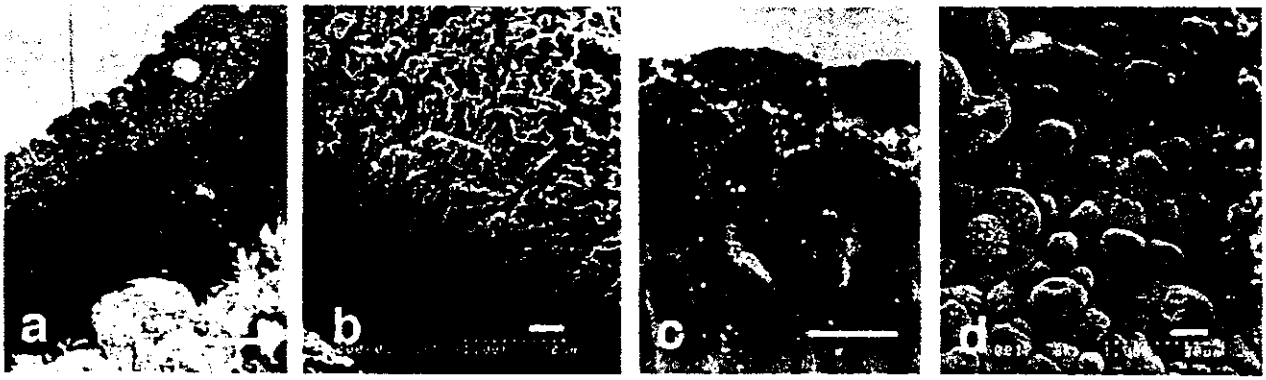

bladder reconstructions using gastrointestinal segments. Gonzalez *et al.* [12] reported a reconstruction technique using seromuscular colocystoplasty lined with urothelium. The seromuscular colonic segment was placed over the urothelial 'bubble' of the bladder the detrusor of which was lifted off the urothelium. Recent advances in tissue-engineering techniques would also potentially allow various new methods of urinary bladder reconstruction, to avoid clinical complications of reconstruction using gastrointestinal flaps [13–15]. However, these approaches have not yet matured for clinical use, for several technical reasons. Meanwhile, covering demucosalized intestinal surface with urothelium grafts obtained from the bladder mucosa or cultured urothelium has been attempted [3–5]. Merguerian *et al.* [3] grafted cultured urothelial cells grown on a biodegradable scaffold onto the demucosalized bowel segment in the rabbit. However, the grafted cells failed to regenerate urothelium. Schaefer *et al.* [4] achieved regenerated urothelium by transplanting cultured urothelium on collagen membranes onto demucosalized gastrointestinal seromuscular segments.

In the present study, cultured canine urothelial cell sheets were grafted successfully onto demucosalized gastric flaps, and a multilayered epithelium regenerated *in vivo*. Aktug *et al.* [5] reported that prefabricating seromuscular flaps partially grafted with urothelium (with no culture) before augmentation cystoplasty helped to avoid the complications caused by intestinal mucosa, and resulted in good bladder capacity. In their method the bladder must be fully opened to obtain large urothelial samples. Cilento *et al.* [16] estimated that it would be theoretically possible to expand a urothelial strain from a single specimen that initially covers a surface area of 1 cm^2 to one covering a surface area of 4202 m^2 within 8 weeks. Using their method of cell culture and our cell-sheet harvesting technology, there is no need to open the bladder for primary culture of urothelium, when small pieces of urothelium can be readily harvested by endoscopy and expanded *in vitro* to cover large seromuscular flaps. If urothelium is taken from the renal pelvis, the engineered flap grafted with cultured urothelial cell sheets can be obtained with no need for bladder biopsy. This is a benefit not only for bladder augmentation but also for whole bladder reconstruction in patients whose bladder must be resected.

Previous work in our laboratory showed that various intact cell sheets from diverse primary sources can be harvested intact with no enzymatic proteolysis (e.g. trypsin or dispase digestion) by using temperature-responsive culture systems [6–8]. To prepare the dish a temperature-responsive polymer, poly(N-isopropylacrylamide), is bonded as a thin overlayer onto commercially available culture dish surfaces using electron beam irradiation [17,18]. This surface is slightly hydrophobic in culture at 37 °C, culturing seeded cells normally, and hydrating spontaneously below 32 °C to become hydrophilic [17,18]. At this reduced temperature, cultured adherent cells spontaneously detach from the rapidly hydrating surface as a single contiguous sheet. Importantly, multilayered or even patterned viable tissue-like cell sheet constructs can be fabricated and transplanted in numerous tissue-regeneration models [19,20].

Urothelial cell sheets were noninvasively harvested by using temperature-responsive culture dishes; proteolytic enzymes (e.g. trypsin or dispase) typically required for cell culture but often destructive to cultured cells can be eliminated [6]. We previously reported that cell-cell junction proteins and extracellular matrix, e.g. cadherin, fibronectin, and laminin, remain intact during such cell-sheet harvest with no enzymes [6–8,21]. These intact cell adhesive proteins facilitate direct, rapid cell-sheet attachment on the demucosalized gastric flap surface. Furthermore, this cell sheet technology has the significant advantage that neither synthetic scaffold nor delivery vehicle is needed to graft the cultured cells *in vivo*. Various delivery vehicles, including collagen sponges, fibrin glue and synthetic biodegradable polymers, have been reported with varying success rates [3,22–24]. A cell-delivery vehicle should have several critical features, including biocompatibility, well-controlled biodegradation, benign cytotoxicity, high affinity for biological integration, and reduced potential for infection. These features are often difficult to obtain. Indeed, cell therapies have limited clinical surgical utility to date, particularly in urological applications. Therefore, the present method which requires no vehicle is better.

Urothelial cell sheets expressed characteristic urothelial uroplakins, while regenerated urothelium on demucosalized gastric flaps did not. Uroplakins are specific molecular markers of the asymmetric unit membrane of urothelium [25]. The structure of the

regenerated epithelium showed squamous metaplasia. Transmission electron microscopy also showed squamous changes in the superficial cell layer of the regenerated epithelium. The most common pathogenic setting for squamous metaplasia is chronic cystitis [26]. Because in the present study the demucosalized gastric flap grafted with urothelial cell sheets was in the abdominal cavity, exposure of its surface to ascites may induce inflammation that resulted in the squamous change.

Li *et al.* [27] reported gastrointestinal mesenchyme/stroma-urothelium interactions; they performed tissue recombination experiments with combinations of rectal mesenchyme and urothelium from embryonic, newborn and adult samples. The tissue recombinants were grafted beneath the kidney capsule of adult male athymic nude mice. The urothelium had the plasticity to change into an intestinal-like epithelium as a result of mesenchymal/stromal stimulation from the gastrointestinal tract. However, they also reported that gastric stromal layers did not induce the transdifferentiation of urothelium [28]; similarly, there was no such transdifferentiation in the present study.

Of the eight urothelial cell sheets autografted in dogs five had viable regenerated epithelium, but three did not. All three demucosalized flaps where urothelial cell sheets were unable to attach had severe surface haematoma. Apparently it is important for cell-sheet attachment to control bleeding from the demucosalized surfaces. The stability of the autografted urothelial cell sheets with no fixation was incomplete in these cases. Additionally, as xenogenic 3T3 feeder cells were used as a feeder layer for *in vitro* culture, an immunologically mediated reaction cannot be excluded [29]. Schaefer *et al.* [4] noted that epithelialization of their demucosalized gastrointestinal surfaces with urothelial cells grown in co-culture with 3T3 feeder cells was more efficient than with urothelial cells grown in monoculture, although they used collagen membranes.

The flaps had shrunk and the smooth muscle was atrophied at death. Both would be caused by lack of stretch, as in the present model there was no augmentation cystoplasty. Currently we are using augmentation cystoplasty with demucosalized intestinal segments covered with cultured urothelial cell sheets.

In conclusion, we confirm that cultured urothelial cell sheets obtained using temperature-responsive culture dishes readily transplant onto demucosalized gastric flaps to produce multilayered epithelium with no glandular epithelial cells *in vivo*. This versatile method should prove useful in urinary tract tissue engineering and surgical reconstruction.

ACKNOWLEDGEMENTS

Dr Kuniko Tsunoyama, Ayako Nishimoto, Shuichi Sekine and Chie Takahashi assisted with surgical procedures. Shigeru Horita, Mayuko Kawashima and Hideki Nakayama provided assistance and advice with electron microscopy interpretation. Dr T.T. Sun (New York University, NY) kindly provided rabbit antiserum to total bovine uroplakins. Prof David W. Grainger (Colorado State University, Ft. Collins, CO USA) provided useful technical comments and editing. The present work was supported by the Japan Society for the Promotion of Science, Grant-in-Aid for Scientific Research (14571524, 13558119) and The Promotion and Mutual Aid Corporation for Private School of Japan.

CONFLICT OF INTEREST

None declared. Source of funding: Japan Society for the Promotion of Science, Grant-in-Aid for Scientific Research (14571524, 13558119).

REFERENCES

Gerharz EW, Turner WH, Kalble T, Woodhouse CR. Metabolic and functional consequences of urinary reconstruction with bowel. *BJU Int* 2003; **91**: 143–9

Mills RD, Studer UE. Metabolic consequences of continent urinary diversion. *J Urol* 1999; **161**: 1057–66

Merguerian P, Chavez DR, Hakim S. Grafting of cultured uroepithelium and bladder mucosa into de-epithelialized segments of colon in rabbits. *J Urol* 1994; **152**: 671–4

Schaefer BM, Lorenz C, Back W *et al.* Autologous transplantation of urothelium into demucosalized gastrointestinal segments: evidence for epithelialization and differentiation of *in vitro* expanded and transplanted urothelial cells. *J Urol* 1998; **159**: 284–90

Aktug T, Ozdemir T, Agartan C, Ozer E, Olguner M, Akgur FM. Experimentally prefabricated bladder. *J Urol* 2001; **165**: 2055–8

Shiroyanagi Y, Yamato M, Yamazaki Y, Toma H, Okano T. Transplantable urothelial cell sheets harvested noninvasively from temperature-responsive culture surfaces by reducing temperature. *Tissue Eng* 2003; **9**: 1005–12

Kushida A, Yamato M, Kikuchi A, Okano T. Two-dimensional manipulation of differentiated Madin-Darby canine kidney (MDCK) cell sheets: the noninvasive harvest from temperature-responsive culture dishes and transfer to other surfaces. *J Biomed Mater Res* 2001; **54**: 37–46

Yamato M, Utsumi M, Kushida A, Konno C, Kikuchi A, Okano T. Thermo-responsive culture dishes allow the intact harvest of multilayered keratinocyte sheets without dispase by reducing temperature. *Tissue Eng* 2001; **7**: 473–80

Hirose M, Kwon OH, Yamato M, Kikuchi A, Okano T. Creation of designed shape cell sheets that are noninvasively harvested and moved onto another surface. *Biomacromolecules* 2000; **1**: 377–81

Rheinwald JG, Green H. Serial cultivation of strains of human epidermal keratinocytes: the formation of keratinizing colonies from single cells. *Cell* 1975; **6**: 331–43

Inoue T, Osatake H. A new drying method of biological specimens for scanning electron microscopy: the t-butyl alcohol freeze-drying method. *Arch Histol Cytol* 1988; **51**: 53–9

Gonzalez R, Buson H, Reid C, Reinberg Y. Seromuscular colocystoplasty lined with urothelium: experience with 16 patients. *Urology* 1995; **45**: 124–9

Kropp BP, Rippy MK, Badylak SF *et al.* Regenerative urinary bladder augmentation using small intestinal submucosa. urodynamic and histopathologic assessment in long-term canine bladder augmentations. *J Urol* 1996; **155**: 2098–104

Probst M, Piechota HJ, Dahiya R, Tanagho EA. Homologous bladder

augmentation in dog with the bladder acellular matrix graft. *BJU Int* 2000; **85**: 362–71

Oberpenning F, Meng J, Yoo JJ, Atala A. De novo reconstitution of a functional mammalian urinary bladder by tissue engineering. *Nat Biotechnol* 1999; **17**: 149–55

Cilento BG, Freeman MR, Schneck FX, Retik AB, Atala A. Phenotypic and cytogenetic characterization of human bladder urothelia expanded *in vitro*. *J Urol* 1994; **152**: 665–70

Yamada N, Okano T, Sakai H, Karikusa F, Sawasaki Y, Sakurai Y. Thermo-responsive polymeric surfaces; control of attachment and detachment of cultured cells. *Makromol Chem Rapid Commun* 1990; **11**: 571–6

Okano T, Yamada N, Sakai H, Sakurai Y. A novel recovery system for cultured cells using plasma-treated polystyrene dishes grafted with poly (*N*-isopropylacrylamide). *J Biomed Mater Res* 1993; **27**: 1243–51

Shimizu T, Yamato M, Isoi Y *et al.* Fabrication of pulsatile cardiac tissue grafts using a novel 3-dimensional cell sheet manipulation technique and temperature-responsive cell culture surfaces. *Circ Res* 2002; **90**: 40

Yamato M, Konno C, Utsumi M, Kikuchi A, Okano T. Thermally responsive polymer-grafted surfaces facilitate patterned cell seeding and co-culture. *Biomaterials* 2002; **23**: 561–7

Kushida A, Yamato M, Konno C, Kikuchi A, Sakurai Y, Okano T. Decrease in culture temperature releases monolayer endothelial cell sheets together with deposited fibronectin matrix from temperature-responsive culture surfaces. *J Biomed Mater Res* 1999; **45**: 355–62

Wechselberger G, Russell RC, Neumeister MW, Schoeller T, Piza-Katzer H, Rainer C. Successful transplantation of three tissue-engineered cell types using capsule induction technique and fibrin glue as a delivery vehicle. *Plast Reconstr Surg* 2002; **110**: 123–9

Atala A, Vacanti JP, Peters CA, Mandell J, Retik AB, Freeman MR. Formation of urothelial structures in vivo from dissociated cells attached to biodegradable polymer scaffolds in vitro. *J Urol* 1992; **148**: 658–62

Tachibana M, Nagamatsu GR, Addonizio JC. Ureteral replacement using collagen sponge tube grafts. *J Urol* 1985; **133**: 866–9

Sun TT, Zhao H, Provet J, Aebi U, Wu XR. Formation of asymmetric unit membrane during urothelial differentiation. *Mol Biol Rep* 1996; **23**: 3–11

Eagan JWJ. Urothelial neoplasms: pathologic anatomy. In Hill GS ed. *Uropathology*, **Vol. II**. New York: Churchill Livingstone, 1989: 719–92

Li Y, Liu W, Hayward SW, Cunha GR, Baskin LS. Plasticity of the urothelial phenotype: effects of gastro-intestinal mesenchyme/stroma and implications for urinary tract reconstruction. *Differentiation* 2000; **66**: 126–35

Master VA, Wei G, Liu W, Cunha GS, Baskin LS. Abstract of Section on Urology, American Academy of Pediatrics. National Conference and Exhibition. Boston, MA, USA 2002: 108–9

Cairns BA, deSerres S, Brady LA, Hultman CS, Meyer AA. Xenogeneic mouse fibroblasts persist in human cultured epidermal grafts: a possible mechanism of graft loss. *J Trauma* 1995; **39**: 75–9

T. Okano, Institute of Advanced Biomedical Engineering and Science, Tokyo Women's Medical University, 8-1 Kawada-cho, Shinjuku-ku, Tokyo, 162-8666, Japan.
e-mail: tokano@abmes.twmu.ac.jp

H&E, haematoxylin and eosin.

Micropatterned surfaces prepared using a liquid crystal projector-modified photopolymerization device and microfluidics

Kazuyoshi Itoga, Masayuki Yamato, Jun Kobayashi, Akihiko Kikuchi, Teruo Okano
Institute of Advanced Biomedical Engineering and Science, Tokyo Women's Medical University, CREST-JST, Kawada-cho 8-1, Shinjuku-ku, Tokyo 162-8666, Japan

Received 17 November 2003; accepted 20 November 2003
Published online 11 March 2003 in Wiley InterScience (www.interscience.wiley.com). DOI: 10.1002/jbm.a.30010

Abstract: A commercial liquid crystal device projector was modified for photopolymerization using its on-board intense light source and a precision optical control circuit. This device projects reduced images generated by a typical personal computer onto the stage where photopolymerization on a surface occurs. This all-in-one device does not require expensive photomasks and external light sources. However, light scattering and diffraction through glass substrates resulted in undesired reactions in areas corresponding to masked (black) domains in mask patterns, limiting pattern resolution. To overcome this shortcoming, two-step surface patterning was developed. First, three-dimensional microstructures of crosslinked silicone elastomer were fabricated with this device and adhered onto silanized glass substrate surfaces, forming microchannels in patterns on the glass support. Then, acrylamide monomer solution containing photoreactive initiator was flowed into these micromold channels and reacted *in situ*. The resultant polyacrylamide layer was highly hydrophilic and repelled protein adsorption. Cell seeding on these patterns in serum-supplemented culture medium produced cells selectively adhered to different patterns: cells attached and spread only on unpolymerized silanized glass surfaces, not on the photopolymerized acrylamide surfaces. This technique should prove useful for inexpensive, rapid prototyping of surface micropatterns from polymer materials. © 2004 Wiley Periodicals, Inc. J Biomed Mater Res 69A: 391–397, 2004

Key words: liquid crystal projector; mask-less pattern formation; microfluidics; cell pattern; cell culture; polydimethylsiloxane (PDMS); polyacrylamide

INTRODUCTION

Soft lithography, first proposed by Whitesides et al.,[1–3] has been widely used for surface micropatterning and other applications. Microstamps for soft lithography templates, usually made of polydimethylsiloxane (PDMS), are conventionally fabricated by semiconductor microfabrication techniques, in which the lithographic preparation of photomask masters is often time-consuming and expensive. Laser ablation is also utilized for the preparation of microstamps,[4,5] and is also less inexpensive. Photopolymerization with standard transparency sheets on which mask patterns were printed by laser printers is another convenient method.[6–9] However, expensive high-end laser printers are required to achieve higher resolution.

Correspondence to: T. Okano; e-mail: tokano@abmes.twmu.ac.jp

Contract grant sponsor: Japan Society for the Promotion of Science; contract grant number: 13308055.
Contract grant sponsor: the Promotion and Mutual Aid Corporation for Private School of Japan, Grants-in-Aid for Scientific Research.

We previously reported a novel photopolymerization device modified from a conventional liquid crystal device projector (LCDP) having an intense light source and precise optical circuit controls.[10] Recent liquid crystal device (LCD) innovation realizes large-scale high-density liquid crystal panels with micrometer scale resolution. The typical pixel size is approximately 20 μm. Such resolution can be useful for micropatterning surfaces in biomedical fields. Furthermore, LCDPs have a well-controlled light source. Projection images can be easily generated using a personal computer (PC) without any special software. Herein, we show preparation of micromolds made of PDMS and surface micropatterning by LCDP photopolymerization utilizing microfluidics. The LCDP-modified device was exploited as a light source and readily accessible photopatterning capabilities.

MATERIALS AND METHODS

Materials

Methacrylate-modified reactive silicone (X-22-164A) was kindly provided by Shin-Etsu Chemical Co. (Tokyo,

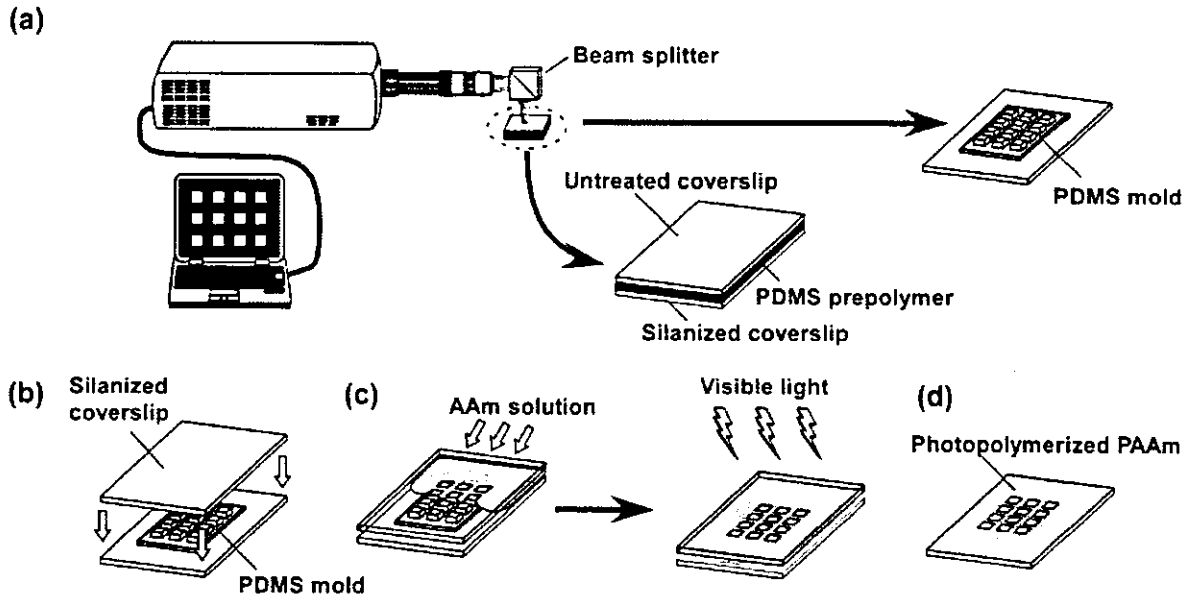

Figure 1. Two-step surface micropatterning utilizing the LCDP-modified photopolymerization device. Three-dimensional PDMS microstructures were prepared for microfluidics patterning on silanized glass surfaces. Micromolded PDMS photopolymerization utilized the LCDP-modified device with designated patterns (a). PDMS microstructures were then placed in contact with silanized glass surfaces as a patterned channel mold (b). Through the mold's open microstructures on the glass surface, acrylamide (AAm) monomer was applied to the coverslip surface, and then LCD light was irradiated with the LCDP-modified device in PC-generated patterns (c). Only in the noncontact PDMS open channel regions, photopolymerization of AAm occurred so that surface micropatterning with PAAm could be achieved (d). Wherever PDMS microstructures contacted the surface, no AAm photopolymerization was observed.

Japan). 3-Methacryloxypropyltrimethoxysilane (MPTMS; Shin-Etsu Chemical Co.), anhydrous methanol (Kanto Chemical Co., Tokyo, Japan), acrylamide, *N,N*-dimethylformamide (DMF), (±)-camphorquinone, *N,N*-dimethyl-*p*-toluidine, anhydrous 1,4-dioxane (Wako Pure Chemical Industries Ltd., Osaka, Japan), fluorescein isothiocyanate (FITC)-labeled bovine serum albumin, rhodamine 123 (both Sigma-Aldrich, St. Louis, MO), and all other chemicals were used as received.

Silane functionalization of glass surfaces

Both sides of glass coverslips (0.2 mm in thickness; Matsunami Glass Inc., Osaka, Japan) were treated by oxygen plasma (irradiation intensity: 400 W; oxygen pressure: 0.1 mmHg) for 180 s in a plasma dry cleaner (PX-1000; SAMCO International, Kyoto, Japan) to clean the surfaces. Plasma-treated coverslips were placed in a separable flask, and dried under vacuum for 30 min. Ten milliliters of MPTMS and 500 mL of anhydrous methanol were poured into the flask under nitrogen gas flow. The coupling reaction of MPTMS with clean, dry coverslip surfaces proceeded under reflux for 24 h at 60°C. The modified coverslips were rinsed repeatedly with methanol and distilled water, and dried for 24 h at 70°C.

Surface micropatterning with polyacrylamide (PAAm) by LCD photopolymerization in PDMS molds

First, surface patterning of PDMS derivatives on the coverslip was performed by irradiation of visible light through patterned images on the liquid crystal panel. A typical preparation procedure follows: camphorquinone (10 mg) as a photopolymerization initiator, and *N,N*-dimethyl-*p*-toluidine (1.0 μL) as a photosensitizer were dissolved in 1.00 g of methacrylate-modified reactive silicone. The solution (6.0 μL) was dropped onto the MPTMS-immobilized coverslip (24 × 24 mm), then covered with an untreated coverslip, creating a liquid film spread uniformly between the coverslips. The set of coverslips was placed in the LCDP apparatus with the untreated coverslip face-forward toward the light source. Visible light LCDP irradiation was performed directly through the top of the untreated coverslip for 20 min. After irradiation, the untreated coverslip was stripped off from the microfabricated PDMS-immobilized on the MPTMS-immobilized coverslip [see Fig. 1(a)]. The resulting PDMS-micropatterned coverslip was repeatedly washed with 1,4-dioxane and acetone to remove unreacted PDMS oligomers.

Second, acrylamide (0.20 g), camphorquinone (10 mg) as the photopolymerization initiator, and *N,N*-dimethyl-*p*-toluidine (1.0 μL) as a photosensitizer were dissolved in 0.80 g of DMF. The MPTMS-immobilized coverslip was then covered with the PDMS-micropatterned coverslip [see Fig. 1(b)],

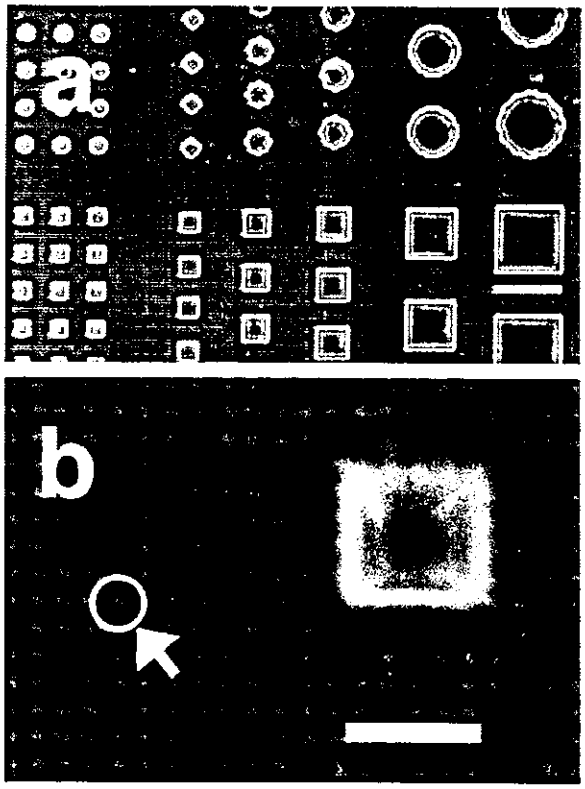

Figure 2. Phase contrast microscopy of three-dimensional PDMS stamp microstructures produced by LCD photopolymerization through the PC-generated mask. Note small gaps among square dots (arrow) caused by the LCD pixel wiring shadows. Scale bar: 200 μm (a); 50 μm (b).

forming patterned microchannels between the two apposing surfaces. The acrylamide solution was poured into the gap of the contacting coverslips and the set of coverslips was irradiated by visible light under a brightness of approximately 50,000 luxes for 4 min [see Fig. 1(c)]. After irradiation, the PDMS-micropatterned coverslip was stripped off, leaving the microfabricated PAAm photoimmobilized on the

Figure 3. SEM of three-dimensional PDMS microstructures. Scale bar: 100 μm.

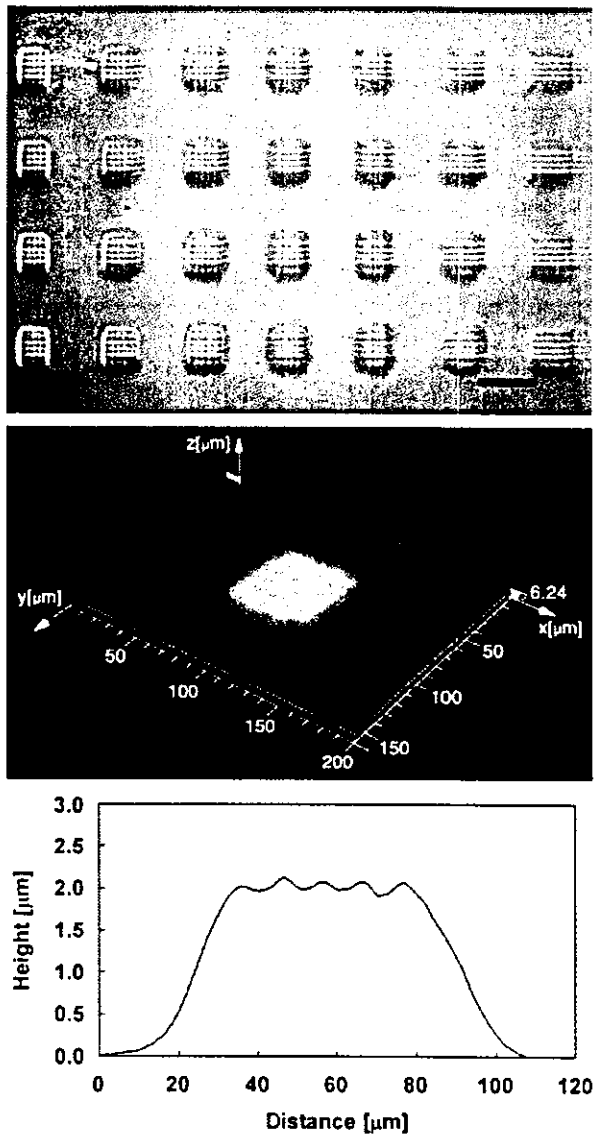

Figure 4. Three-dimensional profiles of three-dimensional PDMS microstructures from laser scanning confocal imaging. Scale bar: 100 μm.

MPTMS-immobilized coverslip in patterns determined by the PDMS micromold. The resulting PAAm-micropatterned coverslip was repeatedly washed with acetone to remove unreacted chemicals.

Micropatterned surfaces were examined under a phase contrast microscope (TE300; Nikon, Tokyo, Japan). Three-dimensional profiles of the surfaces were obtained by reflective confocal laser scanning microscopy (ICM-1000; Leica Microsystems, Wetzlar, Germany). For scanning electron microscopy (SEM) imaging (S-800; Hitachi, Tokyo, Japan), micropatterned surfaces were deposited with a thin conducting gold sputtered layer. Atomic force microscope (AFM) images of patterned PAAm surfaces were obtained with a scanning probe microscope (SPM-9500J3; Shimadzu Corp., Kyoto, Japan) that was operated in dynamic mode in distilled water at ambient temperature.